The Journal of Chemical Physics

RESEARCH ARTICLE | MARCH 07 2025

Insights from virtual chemistry: Shear and bulk viscosity of organic liquids via molecular simulations

Imogen Daisy Smith ; Marcello Sega

J. Chem. Phys. 162, 094502 (2025)
https://doi.org/10.1063/5.0251585

The Journal of Chemical Physics ARTICLE pubs.aip.org/aip/jcp

Insights from virtual chemistry: Shear and bulk viscosity of organic liquids via molecular simulations

Cite as: J. Chem. Phys. 162, 094502 (2025); doi: 10.1063/5.0251585
Submitted: 3 December 2024 • Accepted: 2 February 2025 •
Published Online: 7 March 2025

View Online Export Citation CrossMark

Imogen Daisy Smith and Marcello Sega[a)]

AFFILIATIONS

Department of Chemical Engineering and Sargent Centre for Process Systems Engineering, University College London, Torrington Place, WC1E 7JE London, United Kingdom

[a)]Author to whom correspondence should be addressed: m.sega@ucl.ac.uk

ABSTRACT

Molecular simulations are important tools for predicting the thermophysical properties of liquids, and a rigorous validation of the model potentials is crucial to ensure their reliability for new applications. In the existing literature on empirical force fields, there is an obvious lack of data for shear and bulk viscosity. While experimental or model values for shear viscosity are widely available and represent an excellent benchmark, bulk viscosity is more challenging to measure, and experimental values are available for only a handful of liquids. Here, we present an analysis of both shear and bulk viscosity, calculated from molecular dynamics simulations via the Green–Kubo relations, for over 140 small molecular Newtonian liquids from the Virtual Chemistry database. Therefore, we provide a comprehensive reference for these transport properties for the popular optimized potential for liquid simulations (OPLS) force field and the generalized Amber force field (GAFF).

I. INTRODUCTION

Viscosity is an essential property of fluids, which characterizes their resistance to flow and determines the rate of momentum transport when they are subjected to deformation.[1] The resistance of fluids to shear deformation, known as shear viscosity, η_s, was introduced by Newton to describe the linear relation between shear stress τ_{xy} and rate of strain $\partial v_x/\partial y$ for a laminar flow in direction x,

$$\tau_{xy} = \eta_s \frac{\partial v_x}{\partial y}, \tag{1}$$

where v_x is the fluid velocity component along the x direction. The resistance to volume changes, known as volume, bulk, dilatational, or second viscosity,[2] was first discussed by Stokes[3] but only later considered in the description of energy dissipation in compressible fluids.[4] As momentum is a conserved quantity, its dynamics are governed by the Navier–Stokes equations,

$$\rho\left(\frac{\partial \mathbf{v}}{\partial t} + \mathbf{v}\cdot\nabla\mathbf{v}\right) = -\nabla p + \nabla\cdot\boldsymbol{\tau} + \mathbf{f}, \tag{2}$$

where ρ is the density, p is the (thermodynamic) scalar pressure, $\mathbf{f}$ is the force density, and $\boldsymbol{\tau}$ is the stress. The constitutive equation for the stress of a Newtonian fluid can be expressed as

$$\boldsymbol{\tau} = -p\mathbf{I} + \eta_s\left[\nabla\mathbf{v} + (\nabla\mathbf{v})^{\mathrm{T}} - \mathbf{I}\frac{2}{3}\nabla\cdot\mathbf{v}\right] + \eta_b(\nabla\cdot\mathbf{v})\mathbf{I}, \tag{3}$$

with $\mathbf{I}$ being the identity matrix. This decomposition underlines that η_s is associated with shear deformations only, while η_b (not to be confused with the longitudinal viscosity, $\lambda = \eta_b - 2\eta_s/3$) is only relevant when compressibility plays a role, as in the case of wave propagation, where it is an important contribution to energy dissipation.

Shear viscosity has ubiquitous applications, and well-established and standardized methods exist for measuring it using a range of commercially available viscometers.[5] In the absence of experimental measurements, shear viscosity in liquids can also be predicted using empirical correlations based on group contributions, such as the Joback method.[6] More accurate correlations, similar to those of Hsu *et al.*,[7] predict the experimental

shear viscosity of organic compounds to be within about 4%, also offering an improvement to previous work in its applicability to nitriles, sulfur-containing compounds, and heterocyclics. Group contribution methods, however, tend to perform well on the set used to perform the fit, but the quality of the extrapolation to other compounds or thermodynamic states is not guaranteed.[8] Several accurate interpolating functions exist, including, for example, those used in the NIST database[9] or Yaws' handbook.[10]

Bulk viscosity, on the contrary, is comparatively less well-studied and understood. Bulk viscosity in liquids emerges when the system is temporarily brought out of equilibrium upon compression or expansion, and the relaxation toward equilibrium at the new density involves dissipative mechanisms that can include a rearrangement of the local structure (relatively fast, leading to a small contribution to η_b), a change in internal degrees of freedom such as vibrational or rotational ones (typically slower), or chemical reactions (potentially very slow).[2] The relative magnitude of the bulk viscosity compared to the shear viscosity becomes important in applications involving the dynamics of compressible flows. In addition to the attenuation and dissipation of acoustic sound waves, which is important in medical ultrasound applications,[11] bulk viscosity also plays a role in the behavior and properties of shock waves,[12] where the incorporation of bulk viscosity effects improves predictions of shock wave thickness.[13,14] The experimental determination of the bulk viscosity is considerably more complicated than that of shear viscosity and can be considered part of the fast developing field of longitudinal rheology.[15,16] The techniques used to measure it include sound attenuation measurements[17–19] and stimulated Rayleigh–Brillouin scattering.[20] The bulk viscosity has been measured experimentally for a limited number of state points of a small set of organic liquids,[21–23] including water,[20,24] and over a broader region of the phase state diagram for noble liquids.[25–27] Transport coefficients of fluids, including the shear and bulk viscosity, can be derived using the hard-sphere Enskog theory,[28] albeit this approach is applicable only up to moderate densities. An *ad hoc* modification of the theory, modified Enskog theory,[29,30] incorporates the characteristics of real simple fluids and can predict the transport properties of real fluids using only pressure, volume, and temperature data.[30] Further extensions allow the transport coefficients of polyatomic fluids to be calculated, with an additive contribution from the internal degrees of freedom,[31] but these retain the limitations of the Enskog theory regarding density.

Molecular dynamics simulations offer a valuable alternative route to estimate both viscosities, providing greater insights into the microscopic structure and dynamics while also enabling the investigation of more complex cases, such as solutions. However, the accuracy of the molecular dynamics estimates obviously depends on the quality of the model potentials (also known as force fields). As *ad hoc* potential parameterizations can be done only for a handful of substances, the so-called general, transferable potentials can be used instead for wider explorations of the chemical space, typically at the expense of accuracy. For this reason, and to provide a benchmark for force fields, it is important to test various structural and dynamical properties of model liquids. Systematic investigations of viscosity are still scarce, both in terms of the number of state points and the variety of fluids. However, their frequency has been increasing in recent years, including results on alkanes,[8,32–34] ester + cyclohexane mixtures,[35] amines,[36] perfluoroalkanes,[37] carbon dioxide,[38] ionic liquids,[39,40] aqueous carbohydrates,[41] and electrolytic solutions.[42–44]

This work builds on the foundational study of Caleman *et al.*, who introduced a benchmark set[45] of 146 liquids in order to assess two popular force fields, the Generalized Amber Force Field (GAFF)[46] and the Optimized Potential for Liquid Simulations (OPLS)–All Atom.[47] In their work, Caleman *et al.* computed the density, enthalpy of evaporation, surface tension, static dielectric permittivity, isothermal compressibility, volumetric expansion coefficient, and heat capacity at constant pressure and volume and compared these results with interpolated experimental data. In this study, we use this set of molecular Newtonian liquids and provide a comprehensive database of viscosity values and their associated errors across a range of different temperatures. We provide values of shear viscosity collected from the literature, calculated from an adaptation of the group contribution method of Hsu *et al.*,[7] and calculated using the interpolating functions of Yaws[10] for comparison. In addition, we compute and report the values of the bulk viscosity of these liquids, providing a unique resource for investigating this less well-studied transport property.

II. METHODS

Transport coefficients in the linear response limit can be represented as integrals of autocorrelation functions,[48,49] with the shear and bulk viscosities given by the formulas

$$\eta_s = \frac{V}{k_B T}\int_0^\infty \langle p_{xy}(t)p_{xy}(0)\rangle\, dt, \tag{4}$$

$$\eta_b = \frac{V}{k_B T}\int_0^\infty \langle p'(t)p'(0)\rangle\, dt, \tag{5}$$

where V is the volume of the simulation box, T is the absolute temperature, k_B is the Boltzmann constant, $\langle\cdots\rangle$ is the canonical ensemble average, p_{xy} is an off-diagonal element of the pressure tensor, and p', in the canonical ensemble, is given by[50–52]

$$p'(t) = p(t) - \langle p\rangle - \left(\frac{\partial p}{\partial E}\right)_{V,T}[E(t) - \langle E\rangle], \tag{6}$$

in which

$$V\left(\frac{\partial p}{\partial E}\right)_{V,T} = \frac{V\alpha_p}{C_V\kappa_T} \tag{7}$$

is the Grüneisen ratio,[53] expressed in terms of the coefficient of thermal expansion $\alpha_p = \frac{1}{V}\left(\frac{\partial V}{\partial T}\right)_p$, isothermal compressibility $\kappa_T = -\frac{1}{V}\left(\frac{\partial V}{\partial p}\right)_T$, and heat capacity $C_V = \left(\frac{\partial U}{\partial T}\right)_V$. Note that in the microcanonical ensemble, p' is just the deviation of the scalar pressure from its mean. The term proportional to the Grüneisen ratio can be thought of as a first order correction to the scalar pressure deviation $p - \langle p\rangle$, which subtracts the indirect effect of moving away from the energy shell of the microcanonical case, for which $E = \langle E\rangle$ would hold. This correction affects the scalar pressure only (and, therefore, only the bulk viscosity) because the thermodynamic average of the off-diagonal pressure tensor element p_{xy} vanishes, as does $\left(\frac{\partial p_{xy}}{\partial E}\right)_{V,T}$.

Although the equilibrium approach requires relatively long sampling and is less efficient than non-equilibrium techniques,[54] it

offers a unified framework for calculating both shear and bulk viscosity. In contrast, non-equilibrium methods differ for shear and bulk viscosity,[55] making them less suitable for systematic studies of many liquids.

We performed molecular dynamics simulations with the GROMACS software package, version 2018.3.[56] The molecular topologies and structure files containing the atomic coordinates of the 146 systems were obtained from https://virtualchemistry.org.[45] In all simulations, we used the Nosé–Hoover algorithm for temperature coupling,[57,58] with a time constant of 2 ps, which is in the range of time scales for intermolecular collisions, as recommended by Holian *et al.*[59] We applied analytical long-range dispersion corrections to the pressure and used the particle mesh Ewald method in its smooth variant to compute the electrostatic corrections,[60] with a real space cutoff of 1.1 nm, a relative value of the real space potential at its cutoff of 10^{-5}, and metallic boundary conditions. We ran the simulations in cubic cells under periodic boundary conditions with an integration time step of 0.002 ps. We saved the elements of the pressure tensor and the internal energy to disk at every time step to fully resolve the autocorrelation functions.

We first performed isobaric–isothermal (NpT) simulations to establish the equilibrium density of each chemical with a 2 ns run using the Parrinello–Rahman pressure coupling algorithm[61] with a compressibility of 5×10^{-5} bar^{-1} and a time constant of 1 ps. From this run, we determined the average box size and used this to rescale the input configuration file. We then used the rescaled configuration file to compute 100 ns long trajectories in the canonical (NVT) ensemble, saving the pressure tensor elements to disk every time step. To improve the statistics for the calculation of the autocorrelation functions of the shear viscosity, we averaged over the three independent off-diagonal components of the pressure tensor (xy, yz, and xz). We then established a clear plateau for the viscosity calculations, except in the cases discussed in the results. Correlation functions were computed using a fast Fourier transform approach, which allowed us to avoid time-consuming windowing and use the complete information stored in the pressure tensor time series.

Sampling the pressure tensor at every time step is particularly important in the presence of flexible bonds, which yield strong short-time oscillations in the autocorrelation function. To investigate the effect of these high-frequency oscillations, we simulated formaldehyde both with flexible bonds and as a fully rigid molecule using virtual sites. Note that, although formaldehyde does not exist as a neat liquid, it is still part of the Virtual Chemistry database and is straightforward to model as a rigid molecule, hence our decision to use it as a testbed for the influence of the internal degrees of freedom. Figure 1 shows a comparison of the autocorrelation function of each model (calculated using GAFF) alongside a sliding window average of that of the flexible model. While the rigid model yields a smooth, monotonous autocorrelation, the flexible model displays oscillations due to internal vibrational modes. Averaging out these oscillations using a sliding window results in a filtered signal that closely resembles that of the rigid model, showing that the internal degrees of freedom contribute only a minor part to the Green–Kubo integral. In fact, the flexible model resulted in a shear viscosity of 0.246 ± 0.002 mPa s at 253.15 K, while the rigid model yielded a slightly lower value of 0.228 ± 0.001 mPa s. Although the viscosity difference is modest, it aligns with expectations: flexible bonds are an additional energy dissipation channel during shearing due to intramolecular vibrational modes, resulting in a higher viscosity. In contrast, rigid bonds restrict these dynamic interactions, lowering energy dissipation and viscosity. Given that the force fields considered here are parameterized for flexible bonds, we retained bond flexibility and sampled the autocorrelation functions at every time step to resolve the rapid dynamic fluctuations.

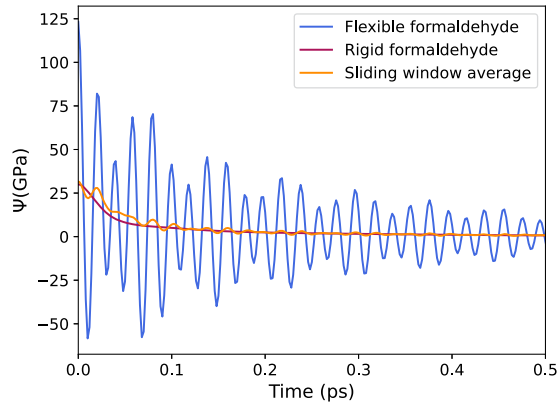

FIG. 1. GAFF shear viscosity autocorrelation function $\Psi(t) = (V/k_BT)\langle p_{xy}(0)p_{xy}(t)\rangle$ for flexible and rigid models of formaldehyde at 253.15 K, along with a sliding window average of the flexible model's autocorrelation function.

To estimate uncertainties of the Green–Kubo running integral, block averaging was used: we split the time series into $M = 10$ non-overlapping blocks of equal size and the integral of the autocorrelation function was computed for each block. The standard error of the mean integral at time t_i is given by $\frac{\sigma(t_i)}{\sqrt{M}}$, where $\sigma(t_i)$ is the standard deviation computed from the blocks, which can be considered completely uncorrelated as they are separated by 10 ns (the largest characteristic decay time of the autocorrelation function we observed was 2.5 ns). Note that here we report only the final estimate of the uncertainty on the transport coefficients, while the error bars on the Green–Kubo running integral are reported only in the dataset available on Zenodo.

In linear response theory, shear and bulk viscosities are evaluated in the limit of infinite time of their respective correlation function cumulative integrals $\eta = \lim_{t\to\infty} \eta(t)$, where we use the symbol η to denote either the shear or the bulk viscosity. In practice, viscosities can be estimated from a plateau at finite time reached by the cumulative integrated correlation functions $\eta(t)$. As the correlation function oscillates around zero for large time lags, the Green–Kubo integral $\eta(t)$ performs a (correlated) random walk around its mean value. Automated plateau detection is challenging because the signal fluctuates significantly at large time lags. To address this problem, we perform a series of fits to a stretched exponential function $A\exp[-(t/\tau)^{\beta}]$ by progressively including larger lags and selecting the optimal upper limit t_f of the fit that minimizes the χ^2. The error estimates $\sigma(t_i)$ from block averaging were used to perform a weighted minimization of the sum of the residuals using the Levenberg–Marquardt algorithm.[62] The viscosity at this point is taken as the result of a subsequent fit to a constant value in the plateau region. While the M blocks are reasonably uncorrelated,

TABLE I. Shear and bulk viscosity calculated using GAFF and the OPLS force field. The shear viscosity data obtained from the literature (Lit.), Yaws' empirical fit (Yaws), and the Hsu *et al.* group contribution method (Group) are reported for comparison (see Table III for experimental bulk viscosity data).

			η_s (mPa s)					η_b (mPa s)		ρ (kg/m^3)	
Molecule	CAS	T (K)	Lit.	Yaws[10]	Group[7]	GAFF	OPLS	GAFF	OPLS	GAFF	OPLS
Acetamide	60-35-5	300.00		14.18	11.08	34(4)	15(1)	17(2)	16(1)	1081.89	1067.21
Acetic-anhydride	108-24-7	300.00		0.77	1.56	4.6(3)	2.5(4)	6.80(9)	5.7(2)	1122.68	1116.79
Acetone	67-64-1	298.15	0.31[64]	0.31	0.29	0.40(1)	0.33(4)	2.8(2)	3.01(9)	786.14	801.02
Acetonitrile	75-05-8	293.15	0.37[65]	0.35	0.37	0.351(8)	0.29(1)	3.46(8)	3.6(1)	736.01	761.54
Acetonitrile	75-05-8	298.15	0.341[66]	0.34	0.35	0.332(6)	0.1583(5)	2.5(2)	3.1(1)	730.11	753.26
Acetophenone	98-86-2	300.00	1.68[a,67]	1.63	1.75	3.3(6)	2.6(5)	10.3(4)	7.1(7)	1020.81	1026.93
2-Aminoethanol	141-43-5	293.15		28.01	3.97	390(3)[b]	6.5(5)	[c]	[c]	1132.59	1026.81
2-Aminoethanol	141-43-5	300.00		20.38	3.41	300(4)[b]	4.7(5)	[c]	[c]	1127.92	1019.58
2-Aminoethanol	141-43-5	320.00	7.577[a,68]	8.98	2.27	[c]	2.40(9)	[c]	[c]	1111.69	997.70
2-Aminoethanol	141-43-5	444.15		0.49	0.37	1.48(3)	0.33(1)	1.36(4)	[c]	1006.00	850.60
Anisole	100-66-3	293.15	1.32[69]	1.09	1.26	1.3(2)	1.2(1)	7(1)	5.4(3)	998.20	987.63
Anisole	100-66-3	298.15	1.06[64]	1.01	1.16	1.2(1)	1.0(1)	6.1(9)	5.28(5)	993.24	982.14
Benzaldehyde	100-52-7	298.15	1.3923[70]	1.39	1.67	2.5(6)	2.3(4)	16.0(7)	8.1(5)	1047.25	1033.67
Benzaldehyde	100-52-7	451.95		0.38	0.39	0.31(3)	0.35(3)	4.93(5)	2.76(9)	884.57	889.02
Benzenethiol	108-98-5	293.15	1.239[71]	1.20	1.50	1.0(1)	0.9(1)	14.0(5)	19.4(8)	1082.74	1070.42
Benzenethiol	108-98-5	298.15	1.144[71]	1.12	1.40	1.0(2)	0.80(7)	11.7(6)	17.7(9)	1076.52	1064.65
Benzonitrile	100-47-0	288.15	1.46[a,72]	1.48	1.44	2.6(5)	1.8(2)	21.9(6)	4.1(2)	1013.30	1013.22
Benzonitrile	100-47-0	300.00	1.12[a,72]	1.22	1.18	1.4(2)	1.6(3)	16.3(8)	3.7(2)	979.69	1003.04
Benzonitrile	100-47-0	464.25		0.29	0.29	0.215(2)	0.1555(8)	4.1(4)	1.018(1)	831.50	849.72
Benzyl-alcohol	100-51-6	297.15	2.13[a,73]	6.04	11.93	4.6(8)	6(1)	6.9(7)	7(2)	1049.45	1044.53
Benzyl-alcohol	100-51-6	300.00	4.90[a,67]	5.35	10.93	3.6(6)	6.0(9)	9(2)	8.0(5)	1044.20	1040.85
1-Bromobutane	109-65-9	293.15	0.63[65]	0.63	0.62	0.61(6)	0.90(8)	5.5(2)	4.8(3)	1189.65	1326.99
1-Bromobutane	109-65-9	298.15	0.61[64]	0.60	0.58	0.57(2)	0.79(3)	5.0(3)	3.7(2)	1182.04	1317.89
Bromoethane	74-96-4	293.15	0.40[65]	0.43	0.39	0.299(4)	0.2856(1)	5.8(3)	7.2(1)	1289.59	1541.79
Bromoethane	74-96-4	298.15	0.37[64]	0.41	0.37	0.29(2)	0.1287(2)	7.0(9)	7.2(3)	1277.50	1530.58
Bromomethane	74-83-9	276.65		0.36	0.34	0.223(5)	0.422(1)	32(3)	30(2)	1402.34	1811.45
Bromomethane	74-83-9	293.15		0.33	0.30	0.187(5)	0.36(2)	19.8(7)	22(1)	1351.58	1762.18
Bromomethane	74-83-9	298.15		0.32	0.29	0.178(5)	0.346(6)	16(1)	24(1)	1329.95	1751.22
1-Bromopropane	106-94-5	293.15	0.52[65]	0.54	0.49	0.48(3)	0.67(1)	5.0(2)	4.2(2)	1240.97	1418.84
1-Bromopropane	106-94-5	298.15	0.49[64]	0.51	0.47	0.420(6)	0.64(1)	4.7(2)	3.90(9)	1231.85	1409.66
1,4-Butanediol	110-63-4	293.15	77.5[74]	95.27	66.43	[c]	[c]	140(8)[b]	[c]	1048.69	1022.65
1,4-Butanediol	110-63-4	298.15	61.7[a,d,74]	73.93	52.89	[c]	[c]	[c]	[c]	1044.89	1019.25
1,4-Butanediol	110-63-4	320.00	23.8[a,d,74]	27.75	20.94	[c]	40(2)[b]	40(4)[b]	[c]	1032.05	1001.26
1-Butanethiol	109-79-5	293.15	0.50[65]	0.54	0.52	0.61(5)	0.65(4)	3.3(3)	3.18(7)	856.74	866.17
1-Butanethiol	109-79-5	298.15		0.51	0.49	0.56(1)	0.58(1)	3.4(1)	3.6(6)	851.48	860.57
1-Butanol	71-36-3	293.15	2.55[65]	2.95	3.10	[c]	2.5(2)	2.7(6)	[c]	820.02	810.44
1-Butanol	71-36-3	298.15	2.5562[75]	2.56	2.71	[c]	2.3(3)	2.3(1)	2.0(5)	816.35	805.43
n-Butylamine	109-73-9	293.15	0.502[76]	0.64	0.49	1.63(6)	0.69(2)	1.72(4)	[c]	780.55	753.02
n-Butylamine	109-73-9	298.15	0.68[69]	0.59	0.46	1.5(1)	0.60(2)	1.59(1)	[c]	774.86	747.04
γ-Butyrolactone	96-48-0	300.00	1.69[a,77]	2.67	1.55	6.1(9)	2.0(2)	19(1)	8.1(4)	1136.13	1099.60
2-Chloroaniline	95-51-2	300.00		2.97	4.46	2.6(3)	3.7(3)	8.8(3)	6.7(6)	1221.34	1228.20
1-Chlorobutane	109-69-3	293.15	0.46[65]	0.43	0.42	0.52(1)	0.46(3)	3.76(7)	3.6(2)	878.00	885.11
1-Chlorobutane	109-69-3	298.15	0.42[64]	0.41	0.40	0.48(3)	0.45(3)	3.8(3)	3.2(2)	871.79	878.79
Chloroethane	75-00-3	273.15		0.32	0.32	0.0442(1)	0.0755(2)	6.60(6)	5.1(2)	899.72	915.69
Chloroethane	75-00-3	285.45		0.29	0.28	0.25(1)	0.26(1)	6.0(2)	4.98(7)	877.00	894.36
Chloroethane	75-00-3	300.00	0.238[a,d,78]	0.26	0.24	0.22(2)	0.22(2)	5.90(8)	4.13(3)	852.89	867.36
2-Chloroethanol	107-07-3	293.15		3.32	4.56	4.1(2)	2.9(1)	2.49(8)	4.11(4)	1229.66	1195.34
2-Chloroethanol	107-07-3	300.00	2.94[a,79]	2.76	3.96	3.5(2)	2.3(1)	2.33(2)	3.7(4)	1221.95	1187.12
2-Chloroethanol	107-07-3	401.75		0.46	0.74	0.60(2)	0.44(3)	1.73(2)	1.37(2)	1098.35	1041.83
1-Chloronaphthalene	90-13-1	300.00	2.59[a,80]	2.72	0.91	2.3(3)	3.5(3)	19.6(7)	21.6(5)	1162.46	1191.19

TABLE I. (*Continued.*)

Molecule	CAS	T (K)	η_s (mPa s) Lit.	Yaws[10]	Group[7]	GAFF	OPLS	η_b (mPa s) GAFF	OPLS	ρ (kg/m^3) GAFF	OPLS
Cyclohexanone	108-94-1	293.15	2.22[65]	2.31	0.15	7(1)	3.6(5)	16.0(1)	9.6(3)	943.80	953.98
Cyclohexanone	108-94-1	298.15	2.02[64]	2.07	0.13	6.2(8)	2.8(4)	15.8(2)	10.8(3)	939.59	949.44
Cyclohexylamine	108-91-8	298.15	1.94[64]	1.81	1.72	110(1)[b]	6(1)	[c]	25(5)	921.48	898.25
Cyclopentanone	120-92-3	293.15	1.17[65]	1.65	0.03	2.3(3)	1.40(5)	11.4(3)	5.3(4)	942.43	948.13
Cyclopentanone	120-92-3	298.15		1.17	0.03	2.2(3)	1.2(2)	10.9(4)	4.6(1)	937.98	942.94
Cyclopropyl-methyl-ketone	765-43-5	293.15		0.96	4.53	1.31(4)	0.86(9)	4.2(4)	3.3(1)	907.25	882.91
Cyclopropyl-methyl-ketone	765-43-5	298.15		0.88	4.31	1.21(3)	0.75(3)	3.9(5)	3.43(3)	902.03	877.89
1,2-Dibromoethane	106-93-4	298.15	1.59[81]	1.62	2.13	0.73(4)	2.78(9)	32(2)	40(3)	1819.18	2352.49
Dibromomethane	74-95-3	293.15	1.02[65]	1.02	2.04	0.46(4)	0.535(4)	5.8(2)	[c]	1963.98	2564.57
Dibromomethane	74-95-3	298.15	0.98[81]	0.97	1.94	0.43(3)	0.77(9)	4.6(5)	[c]	1949.23	2547.04
1,2-Dibromopropane	78-75-1	293.15		1.67		1.04(7)	3.9(4)	10.2(3)	7(1)	1717.23	2112.24
1,2-Dibromopropane	78-75-1	298.15	1.49[69]	1.55		0.97(5)	3.8(5)	12.1(7)	9(1)	1708.51	2103.95
Dibutylamine	111-92-2	293.15	0.95[65]	0.94	0.13	1.84(9)	1.43(6)	3.7(1)	2.99(9)	776.70	775.08
Dibutylamine	111-92-2	298.15	0.92[64]	0.86	0.12	1.60(7)	1.34(5)	3.5(1)	2.32(6)	772.15	769.82
Dibutyl-ether	142-96-1	293.15	0.691[82]	0.64	0.73	1.23(5)	1.2(2)	7.2(3)	3.9(1)	777.85	773.05
Dibutyl-ether	142-96-1	298.15	0.649[a,82]	0.60	0.68	1.09(4)	0.9(1)	4.8(2)	4.2(1)	772.92	767.96
1,4-Dichlorobutane	110-56-5	298.15		0.93	0.92	1.6(2)	1.3(1)	9.0(3)	8.6(5)	1126.76	1130.15
1,1-Dichloroethane	75-34-3	293.15		0.50	0.46	0.46(2)	0.40(2)	9.0(2)	7.0(1)	1177.38	1180.02
1,1-Dichloroethane	75-34-3	298.15	0.46[64]	0.47	0.43	0.304(2)	0.2188(5)	10.4(4)	8.0(2)	1167.73	1172.02
1,2-Dichloroethane	107-06-2	298.15	0.78[64]	0.80	0.69	0.73(2)	0.77(4)	14.4(3)	12(2)	1236.03	1241.01
1,1-Dichloroethene	75-35-4	293.15		0.45	0.49	0.1132(2)	0.31(1)	8.8(3)	10.5(3)	1151.69	1242.42
1,1-Dichloroethene	75-35-4	298.15		0.43	0.46	0.0844(3)	0.30(1)	9.4(3)	11(1)	1142.10	1233.59
Dichlorofluoromethane	75-43-4	300.00	0.26[83]	0.34	0.27	0.203(3)	0.206(6)	[c]	30(1)	1284.73	1309.69
Dichloromethane	75-09-2	293.15	0.435[76]	0.45	0.36	0.33(2)	0.262(8)	7.1(5)	[c]	1268.22	1232.16
Dichloromethane	75-09-2	298.15	0.413[76]	0.43	0.33	0.31(4)	0.241(5)	6.54(1)	[c]	1258.66	1217.35
1,3-Dichloropropane	142-28-9	298.15	0.9443[75]	0.73	0.80	1.03(6)	0.93(3)	10.6(7)	10.5(3)	1165.51	1171.97
Diethanolamine	111-42-2	293.15	889.655[84]	1197.98	49.23	[c]	[c]	[c]	[c]	1162.37	1100.71
Diethanolamine	111-42-2	300.00	494.9[a,84]	648.05	34.59	[c]	[c]	[c]	[c]	1156.93	1096.67
Diethanolamine	111-42-2	320.00	134.0[a,84]	135.60	13.29	[c]	400(1)[b]	[c]	[c]	1156.47	1085.62
Diethanolamine	111-42-2	541.95		0.22		1.07(3)	0.44(2)	1.38(5)	[c]	985.46	861.68
Diethylamine	109-89-7	293.15	0.35[65]	0.33		0.49(2)	0.2168(7)	2.0(3)	1.30(2)	738.72	723.50
Diethylamine	109-89-7	298.15	0.32[64]	0.31		0.432(6)	0.1660(5)	2.0(3)	1.11(1)	732.37	716.93
Diethyl-carbonate	105-58-8	298.15	0.746[85]	0.77	0.72	4.3(2)	1.4(2)	9.0(6)	5.0(9)	1022.06	998.69
Diethylene-glycol	111-46-6	288.15		48.12	31.71	[c]	130(6)[b]	[c]	40(6)	1201.35	1107.81
Diethylene-glycol	111-46-6	293.15	35.73[65]	37.19	25.62	[c]	[c]	[c]	[c]	1199.08	1101.07
Diethylene-glycol	111-46-6	298.15	30.20[64]	29.11	20.89	[c]	[c]	[c]	[c]	1197.39	1096.76
Diethylene-glycol	111-46-6	518.95		0.31	0.15	0.94(2)	0.37(2)	2.0(2)	[c]	1009.42	857.75
Diethyl-malonate	105-53-3	293.15	2.15[65]	1.96	2.12	[c]	4.7(3)	20(2)	6(3)	1098.07	1086.24
Diethyl-malonate	105-53-3	300.00		1.69	1.90	[c]	4.2(2)	16(1)	4.8(5)	1091.67	1079.50
Diethyl-malonate	105-53-3	473.15		0.24	0.21	0.56(1)	0.394(8)	1.006(3)	1.85(3)	916.27	895.89
Diethyl-sulfide	352-93-2	293.15	0.45[65]	0.43	0.45	0.328(4)	0.59(5)	4.3(2)	3.1(1)	815.31	842.31
Diethyl-sulfide	352-93-2	298.15	0.42[64]	0.41	0.42	0.381(8)	0.52(1)	4.0(2)	3.0(2)	809.02	837.23
1,2-Difluorobenzene	367-11-3	293.15		0.66	0.58	0.60(6)	0.71(9)	10.7(6)	14(2)	1108.90	1153.94
1,2-Difluorobenzene	367-11-3	298.15		0.61	0.55	0.58(8)	0.62(8)	10.7(5)	13.2(3)	1101.55	1145.98
1,3-Difluorobenzene	372-18-9	300.00		0.54	0.53	3.6(4)	0.57(9)	10.5(5)	18.4(6)	1060.14	1137.16
Diglyme	111-96-6	293.15	1.06[86]	1.06	0.78	[c]	3.6(5)	2.8(2)	4(1)	1015.37	960.35
Diglyme	111-96-6	298.15		0.98	0.72	[c]	2.6(1)	7(5)	3.1(6)	1010.12	954.37
Diisopropylamine	108-18-9	293.15		0.42	0.10	0.86(4)	0.60(3)	2.9(2)	2.75(6)	768.13	756.51
Diisopropylamine	108-18-9	298.15	0.39[64]	0.40	0.09	0.81(4)	0.519(9)	3.18(3)	2.482(3)	763.25	751.19
Diisopropyl-ether	108-20-3	298.15	0.315[a,82]	0.36	0.26	0.595(1)	0.49(2)	2.42(4)	1.96(5)	763.82	748.38
1,2-Dimethoxybenzene	91-16-7	298.15			2.32	3.4(6)	2.7(4)	6(1)	4.5(5)	1076.32	1058.51

TABLE I. (*Continued.*)

Molecule	CAS	T (K)	η_s (mPa s) Lit.	Yaws[10]	Group[7]	GAFF	OPLS	η_b (mPa s) GAFF	OPLS	ρ (kg/m^3) GAFF	OPLS
Dimethoxymethane	109-87-5	300.00	0.307[a,87]	0.33	0.22	0.47(2)	0.41(1)	4.5(2)	1.67(4)	904.43	871.98
N,N-Dimethylacetamide	127-19-5	300.00		0.83	0.47	1.26(4)	1.30(9)	4.33(5)	3.35(7)	944.68	926.39
N,N-Dimethylformamide	68-12-2	298.15	0.79[64]	0.87	0.80	1.4(2)	0.97(5)	6.1(3)	3.48(7)	986.76	922.54
2,4-Dimethyl-3-pentanone	565-80-0	293.15		0.62	0.76	2.12(8)	1.14(7)	5.16(9)	2.85(5)	822.25	833.42
2,4-Dimethyl-3-pentanone	565-80-0	298.15		0.58	0.70	1.9(2)	1.02(3)	4.9(3)	3.0(1)	817.64	828.86
2,6-Dimethyl-4-heptanone	108-83-8	293.15	1.03[65]	0.96	1.00	1.90(8)	1.81(8)	4.2(5)	4.8(4)	825.29	841.02
2,6-Dimethyl-4-heptanone	108-83-8	298.15		0.88	0.92	1.9(2)	1.69(8)	5.2(2)	5.4(2)	820.85	836.45
Dimethyl-disulfide	624-92-0	293.15		0.59	1.00	0.42(1)	0.58(2)	6.94(3)	4.37(6)	1022.77	1036.94
Dimethyl-disulfide	624-92-0	298.15		0.56	0.94	0.41(1)	0.55(1)	7.51(3)	4.9(3)	1015.18	1030.08
Dimethylether	115-10-6	240.00	0.216[a,d,88]		0.19	0.28(1)	0.23(1)	8.2(4)	2.0(1)	772.84	741.62
Dimethylether	115-10-6	293.15		0.10	0.12	0.17(3)	0.123(2)	3.2(1)	1.06(9)	688.96	650.74
Dimethylether	115-10-6	298.15		0.09	0.12	0.148(8)	0.117(3)	2.98(1)	0.98(8)	680.92	640.49
Dimethyl-sulfide	75-18-3	293.15	0.29[65]	0.29	0.28	0.22(2)	0.35(1)	5.0(3)	3.3(2)	810.13	844.11
Dimethyl-sulfide	75-18-3	298.15	0.28[64]	0.28	0.27	0.0682(1)	0.33(2)	5.7(2)	3.33(6)	801.65	837.28
Dimethyl-sulfoxide	67-68-5	298.15	1.99[64]	2.01	2.41	2.7(3)	2.3(2)	7.0(3)	4.7(3)	1136.64	1101.60
Dimethyl-sulfoxide	67-68-5	462.15		0.35	0.45	0.40(4)	0.396(9)	2.03(5)	1.57(1)	956.03	934.69
1,3-Dioxolane	646-06-0	293.15			37.52	1.48(5)	0.80(2)	18.0(5)	5.5(4)	1122.79	1053.95
1,3-Dioxolane	646-06-0	298.15	0.588[89]		36.36	1.41(7)	0.79(1)	20(1)	6.5(6)	1117.06	1046.15
1,3-Dioxolane	646-06-0	347.15			25.36	0.74(9)	0.41(1)	10.6(6)	3.5(2)	1060.46	977.86
Diphenyl-ether	101-84-8	300.00		3.46	5.23	5.4(8)	[c]	22.5(6)	77(9)[b]	1077.62	1089.03
1,2-Ethanediamine	107-15-3	293.15	1.54[65]	2.29	0.90	16(2)	4.8(3)	7(2)	5.2(2)	1041.72	987.37
1,2-Ethanediamine	107-15-3	298.15		1.96	0.83	11.3(8)	3.7(3)	5.2(2)	16.8(9)	1036.33	981.04
1,2-Ethanedithiol	540-63-6	293.15			1.17	0.9(1)	1.4(1)	6.9(4)	9.9(3)	1173.72	1163.35
1,2-Ethanedithiol	540-63-6	298.15			1.09	0.82(2)	1.4(2)	7.1(2)	12.0(2)	1167.07	1157.72
Ethanol	64-17-5	293.15	1.20[65]	1.15	1.26	1.13(7)	1.00(3)	1.9(2)	1.68(7)	802.77	801.85
Ethanol	64-17-5	298.15	1.07[64]	1.04	1.16	1.09(6)	0.93(3)	1.61(3)	1.6(1)	797.71	796.36
Ethyl-acetate	141-78-6	300.00	0.41[a,90]	0.41	0.40	0.96(4)	0.62(1)	3.3(3)	3.1(2)	929.82	919.78
Ethylene-carbonate	96-49-1	298.15		0.94	13.70	15(1)	4.4(4)	25(1)	15.6(3)	1374.17	1334.29
Ethylene-carbonate	96-49-1	312.15		0.80	12.23	10.3(8)	3.4(3)	17(4)	14.2(5)	1361.24	1320.36
Ethylene-carbonate	96-49-1	521.15		0.36	2.14	0.62(2)	0.425(9)	4.5(1)	4.2(5)	1157.01	1104.69
Ethyl-propanoate	105-37-3	300.00		0.48	0.52	1.08(3)	0.86(6)	3.4(2)	2.63(8)	907.53	906.37
1-Ethylpropylamine	616-24-0	293.15		0.70	0.67	1.71(6)	0.77(2)	[c]	2.3(1)	786.31	772.61
1-Ethylpropylamine	616-24-0	298.15		0.64	0.62	1.40(4)	0.70(4)	[c]	1.9(3)	781.57	766.52
Ethyl-vinyl-ether	109-92-2	300.00		0.23	2.65	0.274(7)	0.29(2)	2.2(1)	1.8(3)	758.42	766.70
Fluorobenzene	462-06-6	293.15	0.60[65]	0.60	0.56	0.56(5)	0.51(1)	[c]	1.986(2)	999.35	1022.54
Fluorobenzene	462-06-6	298.15	0.55[64]	0.56	0.53	0.50(4)	0.48(2)	18.2(5)	2.17(2)	991.60	1015.88
Formaldehyde	50-00-0	253.15		18.28	5.79	0.246(5)	0.260(5)	10.4(3)	1.34(6)	838.99	772.94
Formaldehyde	50-00-0	253.65		16.35	5.77	0.244(4)	0.262(4)	12.0(4)	1.54(5)	838.57	772.38
Formaldehyde	50-00-0	300.00		0.11	4.52	0.152(3)	0.14(2)	6.3(2)	0.950(1)	757.12	703.58
Formamide	75-12-7	298.15	3.23[65]	3.40	3.34	4.0(2)	[c]	3.34(3)	[c]	1218.85	
Formic-acid	64-18-6	293.15		1.88	1.79	16(1)	0.90(6)	[c]	[c]	1397.21	1141.96
Formic-acid	64-18-6	298.15	1.58[91]	1.70	1.61	19(3)	0.80(3)	[c]	[c]	1391.81	1136.36
Furan	110-00-9	293.15	0.38[65]	0.37	1.73	0.50(1)	0.472(9)	21(1)	22.2(5)	974.56	968.09
Furan	110-00-9	298.15	0.36[64]	0.35	1.63	0.46(2)	0.45(1)	17.5(4)	20(2)	967.93	961.45
Glycerol	56-81-5	293.15	1443[a,92]	1064.22	1951.07	[c]	1050(7)[b]	[c]	[c]	1308.29	1259.99
Glycerol	56-81-5	300.00	837.5[a,92]	658.18	1242.84	[c]	[c]	[c]	[c]	1305.23	1255.88
Glycerol	56-81-5	320.00	202.2[a,92]	190.44	385.11	[c]	160(2)[b]	[c]	[c]	1293.83	1235.55
Glycerol	56-81-5	563.15		0.35	0.46	0.469(2)	0.345(1)	[c]	[c]	1083.72	1012.56
2-Heptanone	110-43-0	293.15		0.77	0.81	1.4(2)	1.09(9)	3.2(2)	2.83(6)	814.59	830.71
2-Heptanone	110-43-0	298.15	0.71[64]	0.72	0.76	1.24(4)	1.1(1)	3.7(5)	2.65(5)	810.53	825.68

TABLE I. (*Continued.*)

Molecule	CAS	T (K)	η_s (mPa s) Lit.	Yaws[10]	Group[7]	GAFF	OPLS	η_b (mPa s) GAFF	OPLS	ρ (kg/m^3) GAFF	OPLS
E-hex-2-ene	4050-45-7	293.15		0.28	58.64	0.288(4)	0.36(2)	2.02(3)	1.34(6)	661.82	682.07
E-hex-2-ene	4050-45-7	300.00		0.26	55.61	0.265(5)	0.32(2)	2.00(6)	0.0402(3)	654.31	674.75
2-Hexanone	591-78-6	298.15	0.58[64]	0.64	0.61	0.96(9)	0.71(2)	3.21(8)	2.6(4)	805.08	821.85
2-Iodopropane	75-30-9	293.15	0.73[69]	0.68	0.61	0.61(1)	0.71(3)	6.49(5)	5.6(4)	1619.25	1851.62
2-Iodopropane	75-30-9	298.15	0.65[64]	0.65	0.59	0.58(1)	0.67(2)	5.6(1)	5.2(3)	1607.93	1837.80
Isobutane	75-28-5	243.65	0.30[83]	0.28	0.29	0.41(2)	0.389(8)	3.6(2)	3.30(2)	632.02	643.64
Isopropylamine	75-31-0	293.15	0.38[65]	0.35	0.41	1.09(3)	0.2225(6)	1.34(2)	[c]	774.96	738.68
Isopropylamine	75-31-0	298.15	0.33[64]	0.33	0.38	1.00(3)	0.43(1)	1.77(7)	1.9(1)	769.33	731.24
Isopropylbenzene	98-82-8	300.00		0.71	0.88	0.87(8)	1.28(9)	5.6(3)	6.1(4)	854.65	874.04
Isoquinoline	119-65-3	298.15		3.54	6.87	7.2(1)	[c]	53(1)	[c]	1111.33	1126.46
Isoquinoline	119-65-3	303.15	3.252[93]	3.15	6.33	5.6(8)	[c]	37(1)	[c]	1106.99	1121.80
Isoquinoline	119-65-3	320.00	2.28[a,93]	2.22	4.94	3.9(6)	[c]	41(2)	[c]	1093.41	1109.91
Methanol	67-56-1	293.15	0.60[65]	0.58	0.75	0.54(1)	0.450(7)	1.4(1)	1.3(2)	813.81	782.42
Methanol	67-56-1	298.15	0.54[94]	0.55	0.69	0.51(2)	0.2016(7)	1.17(1)	2.00(8)	808.37	776.38
2-Methyl-2-butanol	75-85-4	293.15	4.63[65]	4.70	4.83	41(8)[b]	4.7(5)	[c]	1.89(5)	839.90	836.67
2-Methyl-2-butanol	75-85-4	298.15		3.72	3.85	[c]	3.6(3)	[c]	1.0(5)	834.60	830.03
2-Methyl-2-butanol	75-85-4	320.00		1.56	1.67	[c]	1.55(5)	[c]	0.7(2)	817.16	805.47
2-Methyl-2-propanol	75-65-0	293.15		5.33	4.35	[c]	8(1)	[c]	[c]	827.98	831.86
2-Methyl-2-propanol	75-65-0	298.15	4.4126[75]	4.12	3.48	[c]	6.8(5)	[c]	[c]	823.62	826.77
2-Methyl-2-propanol	75-65-0	320.00		1.59	1.54	8.9(9)	2.02(1)	2.4(3)	[c]	804.61	801.14
Methyl-acetate	79-20-9	300.00	0.377[a,95]	0.35	0.30	0.69(3)	0.428(5)	5.1(3)	2.83(5)	964.20	943.78
N-Methylacetamide	79-16-3	300.00	4.52[a,96]	4.81	0.90	4.3(4)	2.4(2)	5.3(4)	3.3(1)	987.36	970.71
Methyl-benzoate	93-58-3	298.15	1.86[64]	1.97	1.87	8(1)	3.0(7)	22(1)	10.1(1)	1112.99	1099.53
N-Methylformamide	123-39-7	292.15		1.80	2.24	3.5(1)	1.52(4)	4.4(5)	3.57(5)	1053.63	985.62
N-Methylformamide	123-39-7	298.15	1.68[64]	1.60	2.00	2.9(2)	1.37(4)	5.3(6)	3.54(8)	1047.11	979.71
Methyl-formate	107-31-3	293.15	0.35[65]	0.35	0.31	0.78(6)	0.37(1)	3.5(4)	2.29(8)	1052.15	958.56
Methyl-formate	107-31-3	298.15	0.33[64]	0.33	0.30	0.7(1)	0.349(6)	3.7(3)	2.28(6)	1046.51	952.06
Methyl-methacrylate	80-62-6	298.15		0.56	0.52	1.02(7)	1.22(3)	4.3(3)	3.15(6)	961.22	986.83
Methyl-methacrylate	80-62-6	373.65		0.28	0.26	0.377(7)	0.50(2)	2.30(7)	1.517(8)	872.87	910.26
Methyloxirane	15 448-47-2	298.15			0.84	0.31(1)	0.250(6)	3.2(5)	1.74(7)	803.90	776.04
Methyloxirane	15 448-47-2	307.65			0.74	0.272(8)	0.272(8)	2.8(1)	1.59(4)	790.20	761.33
2-Methylphenol	95-48-7	298.15		7.54	11.11	20(2)	24(4)	15(3)	3(5)	1051.33	1052.47
2-Methylphenol	95-48-7	308.15	5.86[a,97]	5.13	7.51	10(1)	12(1)	6.5(9)	3(3)	1041.77	1042.40
3-Methylphenol	108-39-4	300.00	6.61[a,98,99]	10.76	10.30	[c]	40(2)[b]	[c]	[c]	1038.93	1042.84
4-Methylphenol	106-44-5	298.15		11.93	11.11	4.5(7)	[c]	11.6(8)	21(4)	1025.58	1042.44
4-Methylphenol	106-44-5	313.15	6.661[98]	6.46	6.27	2.7(4)	[c]	7.5(2)	1(1)	1011.32	1029.08
4-Methylphenol	106-44-5	320.00	5.13[a,98]	5.04	4.97	2.5(4)	[c]	6.7(3)	3.4(5)	1004.37	1023.99
4-Methylphenol	106-44-5	475.13		0.36	0.35	0.27(1)	0.43(6)	1.81(8)	1.46(1)	836.47	867.66
2-Methylpyridine	109-06-8	293.15	0.81[65]	0.78	0.86	1.04(7)	1.17(8)	8.0(5)	8.51(8)	951.46	955.62
2-Methylpyridine	109-06-8	298.15		0.73	0.80	0.95(6)	1.10(8)	7.9(4)	7.8(1)	945.55	950.66
3-Methylpyridine	108-99-6	293.15	0.9459[100]	0.96	0.86	1.2(1)	1.4(2)	8.7(5)	10.7(1)	954.85	959.49
3-Methylpyridine	108-99-6	298.15	0.889[a,100]	0.89	0.80	1.1(1)	1.17(8)	9.1(1)	8.9(2)	949.50	954.58
4-Methylpyridine	108-89-4	293.15	0.90[65]	0.92	0.86	1.0(2)	1.3(2)	8.7(6)	9.2(1)	956.29	956.15
4-Methylpyridine	108-89-4	298.15		0.85	0.80	0.97(1)	1.1(2)	10.8(4)	9.1(7)	951.16	951.44
Methyl-salicylate	119-36-8	298.15	2.717[101]	2.33	45.91	80(1)[b]	[c]	[c]	[c]	1220.37	1204.14
Methyl-salicylate	119-36-8	320.00		1.55	18.97	15(2)	5.2(6)	32(3)	14.0(7)	1202.31	1183.16
Methyl-salicylate	119-36-8	496.05		0.33	0.85	0.427(9)	0.46(4)	3.0(2)	1.69(1)	1023.90	1015.40
Morpholine	110-91-8	293.15	2.23[65]	2.22	7.41	[c]	[c]	[c]	[c]	1089.57	1046.05
Morpholine	110-91-8	300.00		1.92	6.61	[c]	10(1)	[c]	[c]	1084.06	1039.18

TABLE I. (*Continued.*)

Molecule	CAS	T (K)	η_s (mPa s) Lit.	Yaws[10]	Group[7]	GAFF	OPLS	η_b (mPa s) GAFF	OPLS	ρ (kg/m^3) GAFF	OPLS
Nitrobenzene	98-95-3	300.00	1.196[a,102]	1.89	0.53	[c]	2.0(4)	17(3)	[c]	1233.82	1177.78
Nitroethane	79-24-3	298.15	0.69[64]	0.66	0.56	2.3(1)	0.79(3)	5.1(3)	3.0(2)	1096.62	1032.33
Nitroethane	79-24-3	387.15		0.30	0.27	0.71(2)	0.310(8)	3.0(2)	1.65(4)	1006.25	913.00
Nitromethane	75-52-5	293.15	0.65[65]	0.67	0.64	2.4(1)	0.66(2)	5.08(5)	3.3(2)	1232.66	1110.91
Nitromethane	75-52-5	298.15		0.63	0.60	2.13(6)	0.63(9)	4.0(4)	4.0(1)	1227.37	1103.68
1-Nitropropane	108-03-2	298.15	0.80[64]	0.79	0.53	3.3(3)	0.96(5)	4.3(7)	4.2(1)	1043.27	989.51
1-Nitropropane	108-03-2	404.25		0.29	0.22	0.72(2)	0.30(2)	1.51(1)	1.4(1)	940.73	857.83
2-Nitropropane	79-46-9	298.15		0.73	0.60	3.4(2)	1.06(6)	6.6(5)	3.28(4)	1036.03	996.73
1-Octanol	111-87-5	298.15	7.5981[103]	7.29	6.89	[c]	110(7)[b]	[c]	[c]	835.09	886.25
1-Octanol	111-87-5	320.00		3.42	3.69	14(2)[b]	40(3)[b]	[c]	[c]	817.33	866.67
Paraldehyde	123-63-7	293.15	1.224[104]	1.19		500(7)[b]	[c]	[c]	[c]	1096.35	1090.47
Paraldehyde	123-63-7	300.00		1.03		110(3)[b]	80(3)[b]	[c]	[c]	1086.23	1085.60
Paraldehyde	123-63-7	397.15		0.29		1.55(8)	1.3(1)	2.75(7)	3.04(2)	994.14	982.71
Pentachloroethane	76-01-7	293.15	2.45[65]	2.42	26.23	1.8(1)	1.9(2)	10.8(4)	[c]	1676.26	1695.71
Pentachloroethane	76-01-7	300.00		2.14	22.96	1.5(2)	1.7(1)	8(2)	[c]	1663.71	1684.77
1,5-Pentanediol	111-29-5	293.15	127.94[65]	139.64	80.11	[c]	[c]	[c]	[c]	1022.10	993.95
1,5-Pentanediol	111-29-5	298.15		107.67	63.46	[c]	[c]	300(1)[b]	[c]	1017.11	990.67
2,4-Pentanedione	123-54-6	298.15		0.75	1.18	2.60(9)	2.8(2)	5.9(1)	3.8(3)	986.44	1016.67
Pentanenitrile	110-59-8	300.00		0.65	0.70	0.94(6)	0.73(2)	4.0(2)	3.38(2)	774.96	781.14
1-Pentanol	71-41-0	293.15	4.00[65]	4.07	4.02	9(1)	4.3(4)	3.5(3)	2.8(3)	825.36	816.75
1-Pentanol	71-41-0	298.15	3.556[85]	3.51	3.50	[c]	3.3(3)	4(2)	2.0(5)	820.79	811.88
1-Pentanol	71-41-0	320.00		1.97	1.99	4.0(4)	1.9(3)	2.3(4)	1(1)	803.59	791.54
3-Pentanol	584-02-1	293.15		5.46	3.84	7.9(9)	4.4(5)	2.6(1)	2.3(2)	821.91	824.87
3-Pentanol	584-02-1	298.15	4.15[64]	4.23	3.24	6.1(5)	3.5(2)	1.27(3)	[c]	817.09	819.58
Phenol	108-95-2	298.15		5.96	8.70	4.9(4)	[c]	13.2(9)	[c]	1080.22	1080.04
Phenol	108-95-2	318.15	4.00[105]	3.79	4.20	2.5(3)	7.7(5)	8.6(7)	[c]	1057.60	1060.81
Propanenitrile	107-12-0	300.00		0.38	0.44	0.51(7)	0.368(5)	4.1(2)	2.8(1)	744.47	750.54
2-Propenenitrile	107-13-1	300.00	0.334[a,106]	0.34	5.44	0.31(3)	0.308(7)	3.77(1)	2.12(5)	761.44	769.54
Propylamine	107-10-8	293.15		0.41	0.36	0.85(2)	0.461(9)	1.39(2)	0.916(7)	764.10	732.90
Propylamine	107-10-8	298.15	0.38[64]	0.38	0.34	0.76(3)	0.45(2)	1.57(9)	1.05(2)	758.08	726.22
Propyne	74-99-7	220.00		0.28	0.43	0.2053(9)	0.194(3)	6.9(3)	15.0(5)	699.00	702.09
Propyne	74-99-7	249.95		0.22	0.30	0.229(9)	0.135(3)	6.3(1)	8.6(7)	657.94	652.75
Pyridine	110-86-1	293.15	0.97[65]	0.95	0.89	1.32(6)	1.2(1)	33(7)	37.1(1)	996.14	984.73
Pyridine	110-86-1	298.15	0.88[64]	0.88	0.83	1.15(8)	1.1(1)	34(5)	31(5)	989.12	978.92
Pyrimidine	289-95-2	293.15			1.83	3.7(5)	2.5(3)	27(2)	39.49(7)	1127.18	1102.56
Pyrimidine	289-95-2	298.15			1.68	3.0(5)	2.5(3)	44(3)	30.6(5)	1121.61	1096.91
Pyrrole	109-97-7	293.15	1.35[65]	1.35	2.33	6.3(5)	1.6(1)	14.4(9)	15(2)	1021.64	991.07
Pyrrole	109-97-7	298.15	1.23[64]	1.23	2.14	5.3(5)	1.46(8)	13(1)	10.8(3)	1017.03	985.96
Pyrrolidine	123-75-1	293.15		0.82	1.61	1.33(7)	0.90(2)	19.5(8)	12.8(3)	1341.90	1301.86
Pyrrolidine	123-75-1	298.15	0.70[64]	0.76	1.43	1.16(3)	0.81(3)	14.6(3)	11(1)	1334.39	1292.42
Quinoline	91-22-5	288.15		4.52	8.20	9(1)	5.8(7)	44(2)	42(4)	1115.37	1099.06
Quinoline	91-22-5	298.15	3.34[64]	3.38	6.87	5.7(8)	4.8(6)	29(8)	45(3)	1106.58	1089.71
Styrene	100-42-5	300.00		0.65	9.14	0.9(1)	0.82(7)	9.6(8)	5.5(3)	898.98	912.95
Sulfolane	126-33-0	291.15			0.62	[c]	[c]	[c]	30(3)[b]	1325.68	1289.31
Sulfolane	126-33-0	300.00	10.98[a,107]		0.57	[c]	100(4)[b]	[c]	[c]	1317.91	1280.60
Sulfolane	126-33-0	320.00	6.80[a,108]		0.48	[c]	30(1)[b]	[c]	26(3)[b]	1301.00	1260.01

TABLE I. (*Continued.*)

Molecule	CAS	T (K)	η_s (mPa s) Lit.	Yaws[10]	Group[7]	GAFF	OPLS	η_b (mPa s) GAFF	OPLS	ρ (kg/m^3) GAFF	OPLS
Sulfolane	126-33-0	473.15			0.13	3.0(4)	1.32(3)	7.0(2)	4.4(1)	1169.65	1105.30
Tert-butylamine	75-64-9	293.15	0.473[109]	0.47	0.70	3.1(2)	0.99(3)	4.0(4)	2.67(7)	783.84	767.92
Tert-butylamine	75-64-9	298.15	0.434[109]	0.43	0.64	2.6(1)	0.88(2)	2.95(5)	2.9(2)	778.75	761.68
1,1,2,2-Tetrachloroethane	79-34-5	293.15	1.50[110]	1.81	1.78	1.06(3)	1.38(5)	24(1)	[c]	1557.41	1598.57
1,1,2,2-Tetrachloroethane	79-34-5	298.15	1.44[111]	1.68	1.60	1.02(7)	1.31(4)	17(1)	[c]	1549.00	1591.25
1,2,3,4-Tetrafluorobenzene	551-62-2	298.15			0.65	0.64(8)	1.0(2)	8.0(4)	11.5(5)	1289.62	1384.38
1,2,3,5-Tetrafluorobenzene	2367-82-0	298.15			0.65	0.49(7)[a]	1.2(2)	7.3(3)	13.0(5)	1276.80	1393.04
Tetrahydrofuran	109-99-9	298.15	0.46[64]	0.46	1.10	0.78(2)	0.53(1)	15.9(7)	5.6(2)	894.64	858.86
Tetrahydrothiophene	110-01-0	293.15	1.04[65]	0.87	0.81	1.26(4)	1.63(1)	14.2(6)	10.1(2)	982.98	987.43
Tetrahydrothiophene	110-01-0	298.15	0.97[64]	0.81	0.76	1.14(5)	1.38(9)	9.7(1)	10.0(7)	976.09	981.77
Thiophene	110-02-1	300.00	0.73[112]	0.59	2.62	0.59(4)	0.96(5)	18.6(8)	21(3)	1050.89	1089.06
Toluene	108-88-3	298.15	0.56[64]	0.56	0.60	0.58(8)	0.80(1)	7(1)	6.1(4)	857.36	874.93
1,1,2-Trichloroethane	79-00-5	293.15		0.96	1.20	0.92(2)	1.10(2)	20.1(8)	24(2)	1426.08	1447.58
1,1,2-Trichloroethane	79-00-5	298.15	1.46[111]	0.88	1.10	0.84(2)	1.05(6)	25(1)	17.0(4)	1418.21	1440.87
Trichloromethane	67-66-3	298.15	0.54[81]	0.53	4.02	0.29(1)	0.292(5)	[c]	[c]	1380.01	1381.42
Triethylamine	121-44-8	293.15	0.36[65]	0.35	0.37	0.58(2)	0.48(2)	3.00(2)	2.2(2)	759.49	749.30
Triethylamine	121-44-8	298.15	0.35[64]	0.33	0.35	0.55(1)	0.47(4)	3.0(2)	2.19(8)	754.38	743.90
Triethyl-phosphate	78-40-0	293.15		1.54		[c]	20(2)	[c]	36(6)	1125.36	1088.00
Triethyl-phosphate	78-40-0	298.15	1.346[a,113]	1.39		[c]	14(2)	[c]	16(2)	1121.93	1081.28
Triethyl-phosphate	78-40-0	320.00		0.96		[c]	6.3(4)	[c]	8(2)	1100.09	1058.07
Trifluoromethyl-benzene	98-08-8	293.15		0.53	0.63	0.8(1)	0.68(1)	8.8(5)	7.6(3)	1199.01	1213.34
Trifluoromethyl-benzene	98-08-8	298.15		0.50	0.59	0.73(8)	0.59(6)	9.5(3)	9.4(2)	1192.02	1205.28
1,2,4-Trimethylbenzene	95-63-6	300.00	0.635[d,114]	0.88	0.83	0.83(7)	1.3(2)	4.70(1)	3.5(2)	859.48	884.51
2,4,6-Trimethylpyridine	108-75-8	295.15		1.27	0.90	1.3(2)	2.0(2)	6.5(2)	8.0(4)	914.28	932.10
2,4,6-Trimethylpyridine	108-75-8	298.15		1.21	0.86	1.3(2)	1.7(2)	6.1(3)	7.1(5)	911.14	929.35
Vinyl-acetate	108-05-4	300.00		0.41	4.85	0.68(1)	0.62(1)	3.6(1)	2.79(8)	977.87	968.82
o-Xylene	95-47-6	293.15	0.81[65]	0.80	0.75	0.9(1)	1.6(2)	5.2(2)	4.9(4)	869.57	891.98
o-Xylene	95-47-6	298.15	0.76[83]	0.74	0.70	0.79(8)	1.4(1)	4.8(2)	5.8(2)	864.88	887.48

[a]Linear interpolation.
[b]Required a 10 ns window.
[c]The stretched exponential fit failed. The uncertainty (one standard deviation) on the last digits is reported in parentheses or, when absent, is half of the last significant digit.
[d]Saturated liquid.

this cannot be said for the values of the Green–Kubo integral separated by small time lag differences. Therefore, to estimate the error in viscosity, we calculated the reduced χ^2 of a constant fit within a window of N_p sampled lags, ranging from 4τ to t_f, out of the total N lags, using an effective number of degrees of freedom,[63]

$$N_{\text{eff}} = \frac{N_p}{1 + 2\sum_{i=1}^{N} R(t_i)}, \tag{8}$$

where $R(t_i)$ is the correlation of $\eta(t)$ at the sampled time lag t_i. This approach worked for most cases, but some needed to be handled separately because of problems in locating the plateau, as detailed in Secs. III and IV.

III. RESULTS

The shear and bulk viscosities calculated using GAFF and the OPLS force field, along with their associated errors for the 146 chemicals at various temperatures, are presented in Tables I. For comparison, available literature results for shear viscosity[64–79,81–114] have been included in the tables under the column "Lit." These are mainly primary experimental data, with the exception of those from compiled references (the CRC Handbooks[64,81]). The available experimental data for bulk viscosity have also been included in Table III [21,115–117] for comparison with the simulated bulk viscosities of a few molecules. In Tables I, shear viscosities obtained using Yaws' interpolated data[10] and the Hsu *et al.* group contribution method[7] are also reported. Yaws' interpolated data serve as the best proxy to systematically test our predictions across all chemicals and temperatures.

Figure 2 reports the correlation plots between Yaws' values ($\eta_{s,\text{Yaws}}$) and those computed using GAFF and the OPLS force field ($\eta_{s,\text{sim}}$), while Fig. 3 presents the correlation between Yaws' values and those calculated with the group contribution method ($\eta_{s,\text{group}}$). For all three methods, the extrapolated values reported in the table were not included in the correlation plots.

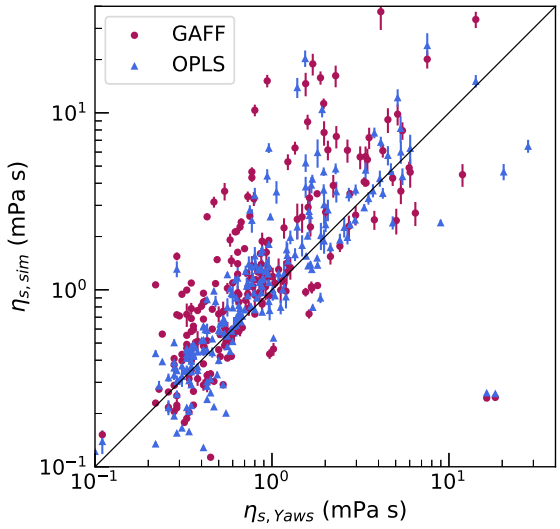

FIG. 2. Correlation between shear viscosity, η_s, calculated using the GAFF (circles), OPLS (triangles) force field, and Yaws' interpolated data.

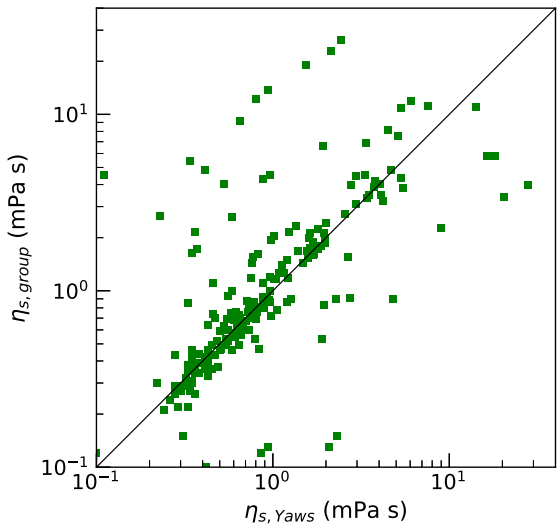

FIG. 3. Correlation between shear viscosity, η_s, calculated using the Hsu *et al.* group contribution method and Yaws' interpolated data.

An important factor to consider when computing the autocorrelation function is the systematic error that arises from the properties of autocorrelations derived from finite datasets. A bias in the autocorrelation estimator occurs due to its requirement for an estimate of its mean.[118,119] This effect was recently brought to our attention by Fitzgerald and Lyman, who formulated an analytical correction for the stretched exponential autocorrelation function.[120] In our case, since we consider the autocorrelation function values only up to a small fraction (1%) of the total simulation length, the calculated bias is negligible.

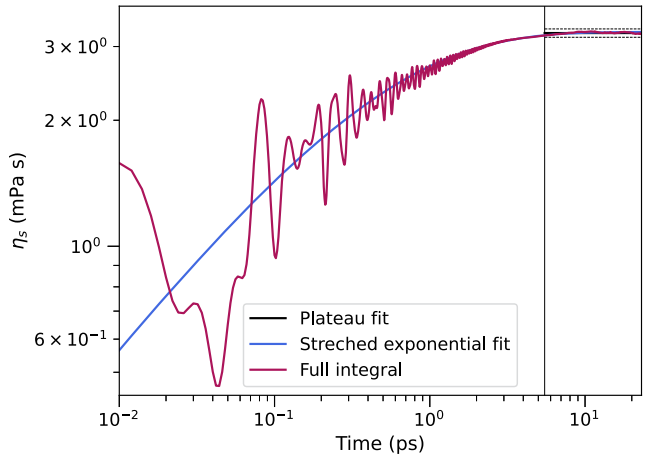

FIG. 4. Green–Kubo integral for the shear viscosity of acetone at 298.15 K, calculated using OPLS. The stretched exponential fit, region for the plateau fit (right of the vertical line), plateau value (solid horizontal line), and plateau uncertainty (dotted lines) are also shown.

We report an example of the Green–Kubo integral in Fig. 4, which shows the case of the shear viscosity for acetone at 298.15 K, calculated using the OPLS force field. The plot features a clearly identified plateau region and data that fit well to a stretched exponential function. In such cases, the approach detailed in Sec. II was used to calculate η_s, finding it here to be 0.323 ± 0.007 mPa s, which shows good agreement with the literature value of 0.31 mPa s.[64]

It is important to note that within this procedure, we perform the stretched exponential fit only to determine the location of the plateau region. Extracting the value of the plateau from the parameters of the stretched exponential may seem tempting, but its

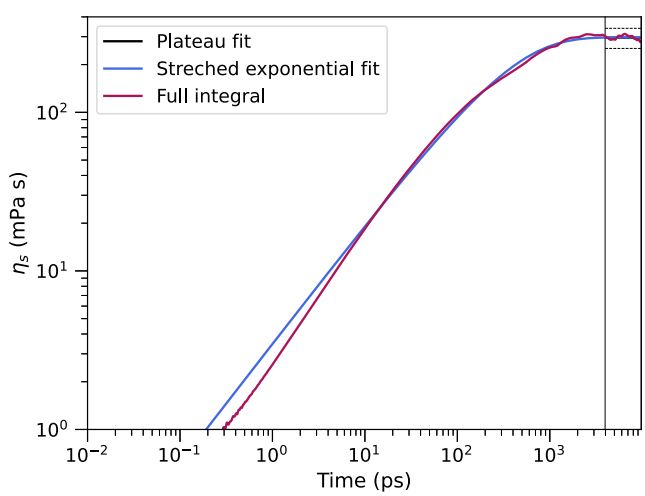

FIG. 5. Green–Kubo integral for the shear viscosity of 2-aminoethanol at 300.0 K, calculated using GAFF, where the automated procedure in the 1 ns window failed due to a relaxation time that was too long. The stretched exponential still fits the Green–Kubo integral well, and a plateau is found.

specific functional form could introduce bias in the estimate. For this reason, we estimate the viscosity by fitting a constant to the plateau region. For most of the molecules in our study, the values for shear and bulk viscosity are well converged, as demonstrated by the small error bars in Fig. 2. However, there were some exceptions, in which a plateau region was not easily defined, and these were handled separately.

When the previously described analysis failed, the data were reanalyzed, extending lags up to 10 ns to see if a clear plateau could be determined. Figure 5 shows the Green–Kubo integral for the shear viscosity, calculated using GAFF in one case, where the automated procedure failed in the 1 ns time lag window but succeeded in the 10 ns one. There are other instances where neither a plateau could be identified nor did the stretched exponential fit the data well: in these cases, we removed the results from the table.

Overall, around 14% of the possible 1096 results for shear or bulk viscosity were discarded due to not being able to confidently determine a plateau value or accept the extrapolated value.

Six molecules had at least one temperature where the results of both force fields were discarded due to the inability to reach the plateau: 1,4-butanediol, diethanolamine, diethylene-glycol, glycerol, morpholine, and 1,5-pentanediol. These molecules share characteristics that may make them prone to developing supercooled or glassy behavior during simulations with the GAFF and OPLS force fields. In particular, 1,4-butanediol, diethanolamine, glycerol, and 1,5-pentanediol contain multiple hydroxyl or amino groups capable of forming extensive hydrogen-bonding networks. Molecules such as glycerol and diols are known for their high viscosity, and even a small inaccuracy in the location of the thermodynamic point in the phase diagram can lead to exponentially growing errors in the estimate of their viscosity; an effectively lower temperature would yield a viscosity high enough to prevent the Green–Kubo integral from reaching a plateau within the simulation timeframe.

One peculiar case where the shear and bulk viscosity results were discarded for both the GAFF and OPLS force fields is 1-octanol. While simulations with GAFF exhibited signatures of supercooled dynamics, the OPLS ones revealed that 1-octanol transitioned into a liquid-crystal phase at both 298.15 and 320 K, possibly the onset of crystallization. In fact, the melting temperature of octanol is known to be overestimated by OPLS.[121] Given that 1-octanol is an important chemical for computing partition coefficients, the failure of both force fields in this study to reliably locate the liquid phase—and, in turn, the viscosity—is significant. It is interesting to note that the water models commonly used to compute partition coefficients with these two force fields[122] show the opposite trend, i.e., their freezing point is shifted toward lower temperatures.[123] This compound effect could be the origin of observed discrepancies in the partition coefficients. It is worth noting that the refined OPLS torsional parameters for aliphatic chains proposed by the group of Böckmann have shown a remarkable improvement in reproducing the shear viscosity of alkanes,[124] and this could, in principle, also benefit aliphatic alcohols.

IV. DISCUSSION

A. Shear viscosity

The overall quality of the shear viscosity predictions by the force fields and group contribution method can be compared by looking at the distributions (shown in Fig. 6) of the relative error (RE) between a predicted value and the corresponding $\eta_{s,\mathrm{Yaws}}$ value and Δ, the absolute error weighted by the estimate's standard deviation (as reported in the tables for the force field calculations, and using 4% for the group contribution method[7]). The distributions appear comparable, with the OPLS force field showing a slightly less pronounced discrepancy with respect to both GAFF and the group contribution method. The slightly better performance of the OPLS force field may be attributed to the fact that it was parameterized specifically for liquid properties, unlike GAFF, which was developed primarily for protein compatibility within the Amber framework—a limitation also noted by Caleman *et al.*[45] These findings highlight the slightly better insight provided by the OPLS force field into the microscopic structure and dynamics of molecular systems. The group contribution method, which relies on broad averages and fixed contributions, generally does a good job, although it struggles with some outliers.

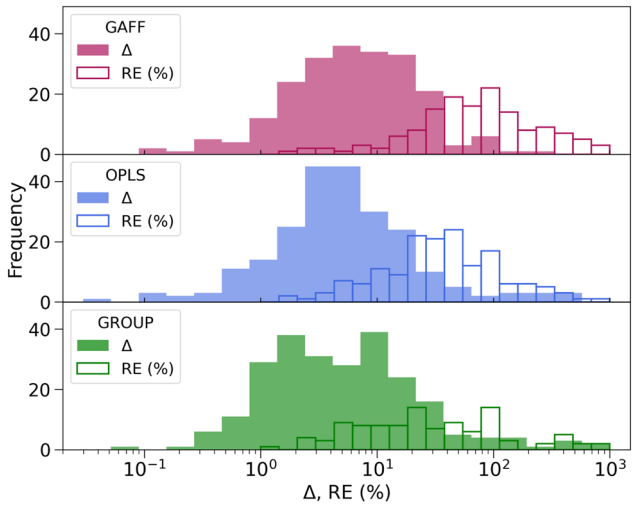

FIG. 6. Histogram of the weighted absolute difference Δ and the relative error (RE) between Yaws' interpolated data[10] and, from top to bottom, GAFF, OPLS, and the Hsu *et al.* group contribution estimates of shear viscosity. The weights are the errors reported in the tables for the force fields and 4% for the group contribution method.[7]

The relative error and the weighted absolute error are both nondimensional quantities that provide complementary information on how well the force fields are performing. This is better illustrated by the bivariate plot of the values of Δ and relative error shown in Fig. 7. We classified chemicals as "poorly modeled" if they exhibit a large relative error (larger than 100%), are more than ten standard deviations away ($\Delta > 10$), and are, therefore, located in the upper right region of the bivariate plot.

The result can be pictorially in Fig. 8, where we report the poorly performing molecules for GAFF and the OPLS force field, as well as those that are not modeled properly by both force fields. We report these molecules in Table II.

For GAFF, one can recognize some groups that appear with some repetition, including the nitro and amino groups. Some esters, alcohols, and diols seem to be problematic both in GAFF and

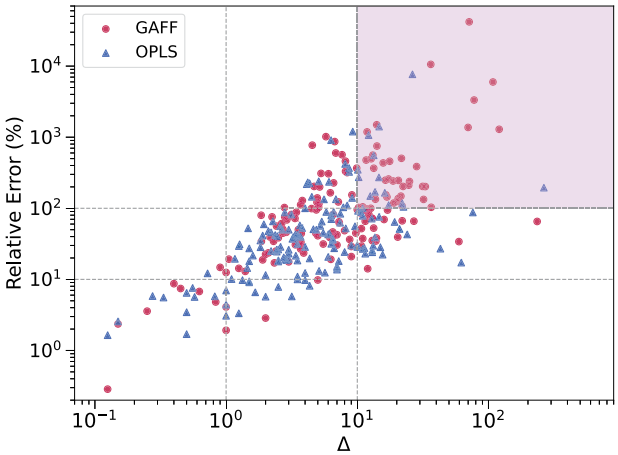

FIG. 7. Correlation between the weighted absolute difference Δ and the relative error for the GAFF and OPLS force field. The molecules in the shaded region (Δ > 10 and relative error RE > 100%) are shown in Fig. 8.

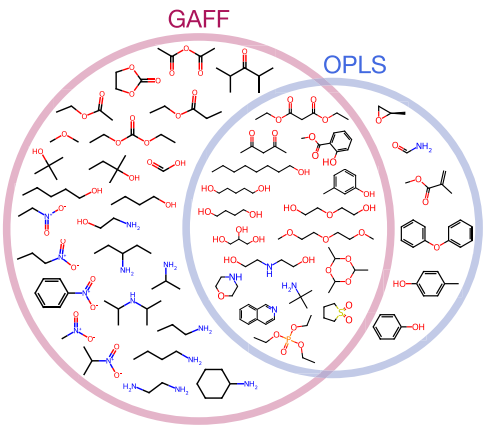

FIG. 8. Molecules that were poorly modeled (Δ > 10 and relative error RE > 100%, which correspond to the top right quadrant in Fig. 7 or whose fit failed) using the GAFF and OPLS force field.

TABLE II. Molecules that were poorly modeled (Δ > 10 and relative error >100%, which correspond to the top right quadrant in Fig. 7 or whose fit failed) using GAFF and the OPLS force field.

GAFF	
Acetic-anhydride	Isoquinoline[a]
2-Aminoethanol	2-Methyl-2-butanol
1,4-Butanediol[a]	2-Methyl-2-propanol
1-Butanol	3-Methylphenol[a]
n-Butylamine	Methyl-salicylate[a]
Cyclohexylamine	Morpholine[a]
Diethanolamine	Nitrobenzene
Diethyl-carbonate	Nitroethane
Diethylene-glycol[a]	Nitromethane
Diglyme[a]	1-Nitropropane
Diethyl-malonate[a]	2-Nitropropane
Diisopropylamine	1-Octanol[a]
2,4-Dimethyl-3-pentanone	Paraldehyde[a]
Dimethylether	1,5-Pentanediol[a]
1,2-Ethanediamine	2,4-Pentanedione[a]
Ethyl-acetate	1-Pentanol
Ethylene-carbonate	Glycerol[a]
Ethyl-propanoate	Propylamine
1-Ethylpropylamine	Sulfolane[a]
Formic-acid	Tert-butylamine[a]
Isopropylamine	Triethyl-phosphate[a]
OPLS	
1,4-Butanediol[a]	Methyl-salicylate[a]
Diethanolamine	Morpholine[a]
Diethylene-glycol[a]	1-Octanol[a]
Diglyme[a]	Paraldehyde[a]
Diethyl-malonate[a]	1,5-Pentanediol[a]
Diphenyl-ether	2,4-Pentanedione[a]
Formamide	Phenol
Isoquinoline[a]	Glycerol[a]
Methyl-methacrylate	Sulfolane[a]
Methyloxirane	Tert-butylamine[a]
3-Methylphenol[a]	Triethyl-phosphate[a]
4-Methylphenol	

[a]Modeled poorly by both GAFF and the OPLS force field.

OPLS, while OPLS has additional issues with some aromatic compounds (anisole, diphenyl ether, and phenols), the only common trait seemingly being an aromatic ring in association with an oxygen substituent. In general, this seems to point to problematic partial charge assignment for oxygen and nitrogen substituents, or possibly missing polarizability effects, as well as inadequate modeling of pi-stacking.

B. Bulk viscosity

One factor that can influence the accuracy of bulk viscosity calculations is the thermostat coupling, which has been shown to introduce oscillations in the Green–Kubo integral. Previous studies, such as those of Hafner *et al.* on water,[52] have shown that these oscillations can be effectively mitigated by using a sufficiently large thermostat time constant. In our simulations, we employ the correction for bulk viscosity and an appropriately large thermostat time constant of 2 ps.

The available literature data for bulk viscosity, on the contrary to shear viscosity, are rather limited, but they confirm a tendency of both force fields to overestimate this transport coefficient. Table III shows a comparison of experimental (Lit.) and simulated (GAFF and OPLS) bulk viscosities for a few molecules. Given the small size of the set, it is hard to say whether the agreement with the experimental values of bulk viscosity is worse than that of shear viscosity.

If one assumes that the molecular mechanisms for energy relaxation during volumetric changes are modeled as well as those responsible for dissipation under shear, one can expect the computer simulation estimates of the bulk viscosity to be as reliable as those of

TABLE III. Comparison of experimental and simulated bulk viscosities.

Molecule	CAS	T (K)	η_b (mPa s) Lit.	GAFF	OPLS
Acetone	67-64-1	298.15	1.4[21]	2.8(2)	3.01(9)
1-Butanol	71-36-3	298.15	3.0[a,115]	2.3(1)	2.0(5)
Butyl acetate	123-86-4	298.15	2.4[21]		
Cyclohexane	110-82-7	298.15	17.4[21]		
Cyclohexanone	108-94-1	298.15	7.0[21]	15.8(2)	10.8(3)
Diethylene-glycol	111-46-6	298.15	49.5[a,116]	[b]	[b]
Ethanol	64-17-5	298.15	1.4[21]	1.61(3)	1.6(1)
Glycerol	56-81-5	293.15	1053[a,117]	[b]	[b]
Glycerol	56-81-5	300.00	729[a,117]	[b]	[b]
Glycerol	56-81-5	320.00	204[a,117]	[b]	[b]
Hexane	110-54-3	298.15	2.4[21]		
Methanol	67-56-1	298.15	0.8[21]	1.17(1)	2.00(8)
3-Methylphenol	108-39-4	300.00	6.2[a,116]	[b]	[b]
1-Pentanol	71-41-0	298.15	2.8[21]	4(2)	2.0(5)
2-Propanol	67-63-0	298.15	2.7[21]		
Pyridine	110-86-1	298.15	62.4[21]	34(5)	31(5)
Toluene	108-88-3	298.15	7.6[21]	7(1)	6.1(4)
Water	7732-18-5	298.15	2.4[21]		

[a]Computed from the ratio of experimental to Stokes' absorption coefficient reported in the cited reference and the experimental viscosity values reported in this work.
[b]The stretched exponential fit failed.

the shear viscosity, since we used the same methodology in a systematic way. In practice, the quality of the bulk viscosity estimates would depend on how well the force field models the local neighborhood of the phase diagram upon volumetric changes: the quality of the isothermal compressibility and volumetric expansion coefficients might give an idea of how well this neighborhood is modeled. The correlation data reported by Caleman *et al.*[45] show that the isothermal compressibility is modeled with a quality similar to that of the shear viscosity reported here, while the volumetric expansion coefficient shows a more pronounced spread. Finally, one should keep in mind that the relaxation modes responsible for the bulk viscosity are, in general, different, or play a different role, than those active under shear. In particular, translational motion and intermolecular collisions are usually dominant in determining the shear viscosity, with rotational modes usually being of secondary importance and vibrational ones being negligible (as shown, for example, in the case of rigid formaldehyde). For bulk viscosity, by contrast, the vibrational modes and the structural relaxations are the most relevant, and electronic degrees of freedom can also play a role.[21,125,126] It is difficult to assess how well the vibrational modes are modeled with OPLS and GAFF, but they could constitute a sizable source of error, especially when the non-harmonicity of chemical bonds comes into play, as the semi-empirical force fields are using harmonic interaction terms. The relaxation of electronic degrees of freedom is also not captured by these force fields, as they do not include atomic polarizability terms. Despite these limitations, the estimates reported in this work represent the largest dataset available on the bulk viscosity of small organic liquids and can be used to investigate bulk viscosity properties in a statistically meaningful way. For example, the bulk viscosity of simple liquids is expected and known to be of the same order of magnitude as the shear viscosity, mostly because the relaxation modes involved in both viscosities are the same, in the absence of, e.g., vibrational degrees of freedom. The bulk viscosities for more complex liquids are expected to be larger than the corresponding shear viscosities, especially if hydrogen bonds are present.

With the data reported here, we can explore this relationship in greater depth. In Fig. 9, we show the correlation between the shear viscosity and the ratio η_b/η_s. This ratio is usually assumed to be of order 1–10. Using our data, we can see that, while this is true in most cases, there are outliers reaching ratios of about 100, and more importantly, there seems to be an inverse correlation between the

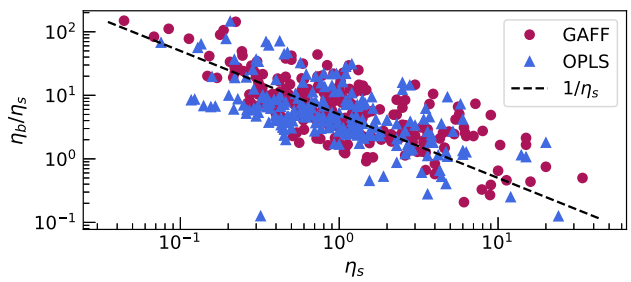

FIG. 9. Correlation between the ratio η_b/η_s and η_s, calculated using the GAFF (circles) and OPLS (triangles) force field. The $1/\eta_s$ scaling is reported as a dashed line.

two quantities, hinting that, in fact, η_b itself might be only mildly correlated with η_s and that it depends on relaxation modes that are different and not strongly correlated with those responsible for the shear viscosity. This result requires further investigation, including understanding if there are multiple distributions of the η_b/η_s ratio associated with distinct molecular properties. However, the simple observation of this correlation highlights the benefit of having a large dataset of bulk viscosity estimates (relative to the available literature data), which can be used for a more systematic statistical analysis.

V. CONCLUSIONS

In this study, we calculated the shear and bulk viscosities of over 140 molecular Newtonian liquids at various state points using GAFF and the OPLS force field, providing reference data and a tool for force field validation and parameterization. Our findings confirm the robustness of the OPLS force field in accurately predicting shear viscosity, demonstrating a strong linear correlation with literature data and, on average, slightly better performance compared to GAFF. This result was not entirely unexpected, as GAFF has not been optimized for bulk liquid properties.

A similar statistically relevant validation for the bulk viscosity is not possible because of the limited available experimental data. However, the force field predictions match the available measurements reasonably well. It is difficult to judge whether inaccuracies should be ascribed to an inaccurate description of the degrees of freedom that are relevant for the bulk viscosity (vibrational, structural, and electronic), the fact that the experimental measurement is not a direct one, or a combination of both. Nevertheless, considering the good match with the available data, we expect the inaccuracy of our bulk viscosity estimates to be in line with, or only slightly larger than, that of the shear viscosity ones.

In conclusion, the data reported here are, to our knowledge, the largest available dataset of shear and bulk viscosities of molecular liquids calculated with empirical force fields and by far the largest dataset of bulk viscosities estimated by any means. It is our hope that this could prompt investigations of the relation between the bulk viscosity of these liquids and the corresponding molecular structure and thermodynamic and transport properties, as well as further experimental investigations. From a computational perspective, it would be interesting to explore the effects of polarizable force fields, which model electronic relaxation modes, as well as anharmonic bending terms that could more accurately account for vibrational relaxation dynamics.

ACKNOWLEDGMENTS

The authors acknowledge the use of the SIGH cluster at the UCL Chemical Engineering Department and the UCL Myriad High Performance Computing Facility (Myriad@UCL) and associated support services, in the completion of this work.

AUTHOR DECLARATIONS

Conflict of Interest

The authors have no conflicts to disclose.

Author Contributions

Imogen Daisy Smith: Investigation (equal); Methodology (equal); Writing – original draft (equal). **Marcello Sega**: Conceptualization (lead); Investigation (equal); Methodology (equal); Writing – original draft (equal).

DATA AVAILABILITY

The data that support the findings of this study are openly available in Zenodo at http://doi.org/10.5281/zenodo.14267059, reference number 14267059.

REFERENCES

[1] R. Bird, W. Stewart, and E. Lightfoot, *Transport Phenomena*, 2nd ed. (Wiley, 2007).
[2] L. D. Landau and E. M. Lifshitz, *Fluid Mechanics*, 2nd ed. (Pergamon Press, Oxford, England, 1989).
[3] G. G. Stokes, "On the effect of the internal friction of fluids on the motion of pendulums," Trans. Cambridge Philos. Soc. **9**, 8 (1850).
[4] L. Tisza, "Supersonic absorption and Stokes' viscosity relation," Phys. Rev. **61**, 531–536 (1942).
[5] D. S. Viswanath, T. K. Ghosh, D. H. Prasad, N. V. Dutt, and K. Y. Rani, *Viscosity of Liquids: Theory, Estimation, Experiment, and Data* (Springer, Dordrecht, The Netherlands, 2007).
[6] K. G. Joback and R. C. Reid, "Estimation of pure-component properties from group-contributions," Chem. Eng. Commun. **57**, 233–243 (1987).
[7] H.-C. Hsu, Y.-W. Sheu, and C.-H. Tu, "Viscosity estimation at low temperatures ($T_r < 0.75$) for organic liquids from group contributions," Chem. Eng. J. **88**, 27–35 (2002).
[8] R. A. Messerly, M. C. Anderson, S. M. Razavi, and J. R. Elliott, "Improvements and limitations of Mie λ-6 potential for prediction of saturated and compressed liquid viscosity," Fluid Phase Equilib. **483**, 101–115 (2019).
[9] M. L. Huber, E. W. Lemmon, I. H. Bell, and M. O. McLinden, "The NIST REFPROP database for highly accurate properties of industrially important fluids," Ind. Eng. Chem. Res. **61**, 15449–15472 (2022).
[10] C. L. Yaws, *Yaws' Handbook of Thermodynamic and Physical Properties of Chemical Compounds* (Knovel, 2003).
[11] S. L. Garrett, *Understanding Acoustics: An Experimentalist's View of Sound and Vibration*, *Graduate Texts in Physics* (Springer International Publishing, Cham, 2020).
[12] R. Boukharfane, P. J. M. Ferrer, A. Mura, and V. Giovangigli, "On the role of bulk viscosity in compressible reactive shear layer developments," Eur. J. Mech., B/Fluids **77**, 32–47 (2019).
[13] A. Claycomb and R. Greendyke, "Extending CFD modeling to the transition regime by enhanced thermophysical modeling," in *40th Thermophysics Conference, Fluid Dynamics and Co-Located Conferences* (American Institute of Aeronautics and Astronautics, 2008).
[14] S. Kosuge and K. Aoki, "Shock-wave structure for a polyatomic gas with large bulk viscosity," Phys. Rev. Fluids **3**, 023401 (2018).
[15] A. Dukhin, "Rheology in longitudinal (ultrasound) mode. Review," Colloid J. **83**, 1–19 (2021).
[16] B. Schroyen, D. Vlassopoulos, P. Van Puyvelde, and J. Vermant, "Bulk rheometry at high frequencies: A review of experimental approaches," Rheol. Acta **59**, 1–22 (2020).
[17] J. Pinkerton, "A pulse method for the measurement of ultrasonic absorption in liquids: Results for water," Nature **160**, 128–129 (1947).
[18] J. R. Pellam and J. Galt, "Ultrasonic propagation in liquids: I. Application of pulse technique to velocity and absorption measurements at 15 megacycles," J. Chem. Phys. **14**, 608–614 (1946).
[19] D. G. Naugle, "Excess ultrasonic attenuation and intrinsic-volume viscosity in liquid argon," J. Chem. Phys. **44**, 741–744 (1966).

[20] X. He, H. Wei, J. Shi, J. Liu, S. Li, W. Chen, and X. Mo, "Experimental measurement of bulk viscosity of water based on stimulated Brillouin scattering," Opt. Commun. **285**, 4120–4124 (2012).
[21] A. Dukhin and P. Goetz, "Bulk viscosity and compressibility measurement using acoustic spectroscopy," J. Chem. Phys. **130**, 124519 (2009).
[22] J. R. Singer, "Excess ultrasonic attenuation and volume viscosity in liquid methane," J. Chem. Phys. **51**, 4729–4733 (1969).
[23] G. Prangsma, A. H. Alberga, and J. J. M. Beenakker, "Ultrasonic determination of the volume viscosity of N_2, CO, CH_4 and CD_4 between 77 and 300 K," Physica **64**, 278–288 (1973).
[24] M. J. Holmes, N. G. Parker, and M. J. W. Povey, "Temperature dependence of bulk viscosity in water using acoustic spectroscopy," J. Phys.: Conf. Ser. **269**, 012011 (2011).
[25] D. G. Naugle, J. H. Lunsford, and J. R. Singer, "Volume viscosity in liquid argon at high pressures," J. Chem. Phys. **45**, 4669–4676 (1966).
[26] W. M. Madigosky, "Density dependence of the bulk viscosity in argon," J. Chem. Phys. **46**, 4441–4444 (1967).
[27] R. S. Chatwell and J. Vrabec, "Bulk viscosity of liquid noble gases," J. Chem. Phys. **152**, 094503 (2020).
[28] S. Chapman and T. Cowling, *The Mathematical Theory of Non-Uniform Gases*, 3rd ed. (Cambridge University Press, London, 1970), Chap. 16.
[29] J. Hirschfelder, C. Curtiss, and R. Bird, *Molecular Theory of Gases and Liquids* (John Wiley & Sons, New York, 1954), Chap. 9.
[30] H. Hanley, R. McCarty, and E. Cohen, "Analysis of the transport coefficients for simple dense fluid: Application of the modified Enskog theory," Physica **60**, 322–356 (1972).
[31] H. J. M. Hanley and E. G. D. Cohen, "Analysis of the transport coefficients for simple dense fluids: The diffusion and bulk viscosity coefficients," Physica A **83**, 215–232 (1976).
[32] N. D. Kondratyuk and V. V. Pisarev, "Calculation of viscosities of branched alkanes from 0.1 to 1000 MPa by molecular dynamics methods using compass force field," Fluid Phase Equilib. **498**, 151–159 (2019).
[33] M. Fischer, G. Bauer, and J. Gross, "Transferable anisotropic united-atom Mie (TAMie) force field: Transport properties from equilibrium molecular dynamic simulations," Ind. Eng. Chem. Res. **59**, 8855–8869 (2020).
[34] S. Schmitt, F. Fleckenstein, H. Hasse, and S. Stephan, "Comparison of force fields for the prediction of thermophysical properties of long linear and branched alkanes," J. Phys. Chem. B **127**, 1789–1802 (2023).
[35] N. V. Sastry, S. R. Patel, and S. S. Soni, "Excess molar volumes, excess isentropic compressibilities, excess viscosities, relative permittivity and molar polarization deviations for methyl acetate+, ethyl acetate+, butyl acetate+, isoamyl acetate+, methyl propionate+, ethyl propionate+, ethyl butyrate+, methyl methacrylate+, ethyl methacrylate+, and butyl methacrylate + cyclohexane at T = 298.15 and 303.15 K," J. Mol. Liq. **183**, 102–112 (2013).
[36] G. A. Orozco, C. Nieto-Draghi, A. D. Mackie, and V. Lachet, "Transferable force field for equilibrium and transport properties in linear, branched, and bifunctional amines I. Primary amines," J. Phys. Chem. B **115**, 14617–14625 (2011).
[37] C. McCabe, D. Bedrov, O. Borodin, G. D. Smith, and P. T. Cummings, "Transport properties of perfluoroalkanes using molecular dynamics simulation: Comparison of united- and explicit-atom models," Ind. Eng. Chem. Res. **42**, 6956–6961 (2003).
[38] F. Jaeger, O. K. Matar, and E. A. Müller, "Bulk viscosity of molecular fluids," J. Chem. Phys. **148**, 174504 (2018).
[39] K. Goloviznina, J. N. Canongia Lopes, M. Costa Gomes, and A. A. Pádua, "Transferable, polarizable force field for ionic liquids," J. Chem. Theory Comput. **15**, 5858–5871 (2019).
[40] D. Bedrov, J.-P. Piquemal, O. Borodin, A. D. MacKerell, Jr., B. Roux, and C. Schröder, "Molecular dynamics simulations of ionic liquids and electrolytes using polarizable force fields," Chem. Rev. **119**, 7940–7995 (2019).
[41] S. H. Jamali, T. v. Westen, O. A. Moultos, and T. J. Vlugt, "Optimizing nonbonded interactions of the OPLS force field for aqueous solutions of carbohydrates: How to capture both thermodynamics and dynamics," J. Chem. Theory Comput. **14**, 6690–6700 (2018).
[42] I. M. Zeron, J. L. F. Abascal, and C. Vega, "A force field of Li^+, Na^+, K^+, Mg^{2+}, Ca^{2+}, Cl^-, and SO_4^{2-} in aqueous solution based on the TIP4P/2005 water model and scaled charges for the ions," J. Chem. Phys. **151**, 134504 (2019).
[43] S. Blazquez, M. Conde, and C. Vega, "Scaled charges for ions: An improvement but not the final word for modeling electrolytes in water," J. Chem. Phys. **158**, 054505 (2023).
[44] A. Z. Panagiotopoulos, "Simulations of activities, solubilities, transport properties, and nucleation rates for aqueous electrolyte solutions," J. Chem. Phys. **153**, 010903 (2020).
[45] C. Caleman, P. J. van Maaren, M. Hong, J. S. Hub, L. T. Costa, and D. van der Spoel, "Force field benchmark of organic liquids: Density, enthalpy of vaporization, heat capacities, surface tension, isothermal compressibility, volumetric expansion coefficient, and dielectric constant," J. Chem. Theory Comput. **8**, 61–74 (2012).
[46] J. Wang, R. M. Wolf, J. W. Caldwell, P. A. Kollman, and D. A. Case, "Development and testing of a general amber force field," J. Comput. Chem. **25**, 1157–1174 (2004).
[47] W. L. Jorgensen and J. Tirado-Rives, "Potential energy functions for atomic-level simulations of water and organic and biomolecular systems," Proc. Natl. Acad. Sci. U. S. A. **102**, 6665–6670 (2005).
[48] M. S. Green, "Markoff random processes and the statistical mechanics of time-dependent phenomena. II. Irreversible processes in fluids," J. Chem. Phys. **22**, 398–413 (1954).
[49] R. Kubo, "Statistical-mechanical theory of irreversible processes. I. General theory and simple applications to magnetic and conduction problems," J. Phys. Soc. Jpn. **12**, 570–586 (1957).
[50] E. Helfand, "Transport coefficients from dissipation in a canonical ensemble," Phys. Rev. **119**, 1–9 (1960).
[51] R. Zwanzig, "Frequency-dependent transport coefficients in fluid mechanics," J. Chem. Phys. **43**, 714–720 (1965).
[52] R. Hafner, G. Guevara-Carrion, J. Vrabec, and P. Klein, "Sampling the bulk viscosity of water with molecular dynamics simulation in the canonical ensemble," J. Phys. Chem. B **126**, 10172–10184 (2022).
[53] O. L. Anderson, "The Grüneisen ratio for the last 30 years," Geophys. J. Int. **143**, 279–294 (2000).
[54] B. Hess, "Determining the shear viscosity of model liquids from molecular dynamics simulations," J. Chem. Phys. **116**, 209–217 (2002).
[55] W. G. Hoover, A. J. Ladd, R. B. Hickman, and B. L. Holian, "Bulk viscosity via nonequilibrium and equilibrium molecular dynamics," Phys. Rev. A **21**, 1756 (1980).
[56] M. J. Abraham, T. Murtola, R. Schulz, S. Páll, J. C. Smith, B. Hess, and E. Lindahl, "GROMACS: High performance molecular simulations through multi-level parallelism from laptops to supercomputers," SoftwareX **1–2**, 19–25 (2015).
[57] S. Nosé, "A molecular dynamics method for simulations in the canonical ensemble," Mol. Phys. **52**, 255–268 (1984).
[58] W. G. Hoover, "Canonical dynamics: Equilibrium phase-space distributions," Phys. Rev. A **31**, 1695–1697 (1985).
[59] B. L. Holian, A. F. Voter, and R. Ravelo, "Thermostatted molecular dynamics: How to avoid the Toda demon hidden in Nosé-Hoover dynamics," Phys. Rev. E **52**, 2338–2347 (1995).
[60] U. Essmann, L. Perera, M. L. Berkowitz, T. Darden, H. Lee, and L. G. Pedersen, "A smooth particle mesh Ewald method," J. Chem. Phys. **103**, 8577–8593 (1995).
[61] M. Parrinello and A. Rahman, "Polymorphic transitions in single crystals: A new molecular dynamics method," J. Appl. Phys. **52**, 7182–7190 (1981).
[62] K. Levenberg, "A method for the solution of certain non-linear problems in least squares," Q. Appl. Math. **2**, 164–168 (1944).
[63] U. Wolff, "Monte Carlo errors with less errors," Comput. Phys. Commun. **156**, 143–153 (2004).
[64] *CRC Handbook of Chemistry and Physics*, 95th ed., edited by W. M. Haynes (CRC Press, Boca Raton, 2014).
[65] A. R. Katritzky, K. Chen, Y. Wang, M. Karelson, B. Lucic, N. Trinajstic, T. Suzuki, and G. Schüürmann, "Prediction of liquid viscosity for organic compounds by a quantitative structure–property relationship," J. Phys. Org. Chem. **13**, 80–86 (2000).

[66]K. Hickey and W. E. Waghorne, "Viscosities and volumes of dilute solutions of formamide in water + acetonitrile and for formamide and *N*,*N*-dimethylformamide in methanol + acetonitrile mixed solvents: Viscosity *B*-coefficients, activation free energies for viscous flow, and partial molar volumes," J. Chem. Eng. Data **46**, 851–857 (2001).
[67]P. S. Nikam and S. J. Kharat, "Densities and viscosities of binary mixtures of *N*,*N*-dimethylformamide with benzyl alcohol and acetophenone at (298.15, 303.15, 308.15, and 313.15) K," J. Chem. Eng. Data **48**, 1291–1295 (2003).
[68]J. Águila-Hernández, A. Trejo, B. E. García-Flores, and R. Molnar, "Viscometric and volumetric behaviour of binary mixtures of sulfolane and *N*-methylpyrrolidone with monoethanolamine and diethanolamine in the range 303–373 K," Fluid Phase Equilib. **267**, 172–180 (2008).
[69]D. Velzen, R. Cardozo, and H. Langenkamp, "Liquid viscosity and chemical constitution of organic compounds: A new correlation and a compilation of literature data," Technical Report No. EUR 4735 e, Commission of the European Communities, Luxembourg, 1972.
[70]M. N. Roy, R. K. Das, and A. Bhattacharjee, "Density and viscosity of acrylonitrile + cinnamaldehyde, + anisaldehyde, and + benzaldehyde at (298.15, 308.15, and 318.15) K," J. Chem. Eng. Data **53**, 1431–1435 (2008).
[71]J. Morris, W. Lanum, R. Helm, W. Haines, G. Cook, and J. Ball, "Purification and properties of ten organic sulfur compounds," J. Chem. Eng. Data **5**, 112–116 (1960).
[72]S. L. Whittenburg and C. Wang, "Light scattering studies of transverse sound wave and molecular motion in benzonitrile," J. Chem. Phys. **66**, 4995–5000 (1977).
[73]K.-D. Chen, Y.-F. Lin, and C.-H. Tu, "Densities, viscosities, refractive indexes, and surface tensions for mixtures of ethanol, benzyl acetate, and benzyl alcohol," J. Chem. Eng. Data **57**, 1118–1127 (2012).
[74]G. Czechowski, P. Jarosiewicz, A. Rabiega, and J. Jadżyn, "The viscous properties of diols. IV. 1,2- and 1,4-butanediol in butanols solutions," Z. Naturforsch. A **59**, 119–123 (2004).
[75]C. Lafuente, H. Artigas, M. C. López, F. M. Royo, and J. S. Urieta, "Viscosimetric study of binary mixtures of 1,3-dichloropropane with isomeric butanols," J. Mol. Liq. **62**, 199–208 (1994).
[76]I. L. Acevedo and M. Katz, "Viscosities and thermodynamics of viscous flow of some binary mixtures at different temperatures," J. Solution Chem. **19**, 1041–1052 (1990).
[77]D. H. Ramkumar and A. P. Kudchadker, "Mixture properties of the water + γ-butyrolactone + tetrahydrofuran system. Part 1: Densities of γ-butyrolactone + water at 303.15–343.15 K and of tetrahydrofuran + γ-butyrolactone at 278.15–298.15 K; and ultrasonic velocities at 298.15 K for the three binary systems inclusive of tetrahydrofuran + water and the ternary system tetrahydrofuran + water + γ-butyrolactone," J. Chem. Eng. Data **34**, 459–463 (1989).
[78]W. Rutherford, "Viscosity and density of some lower alkyl chlorides and bromides," J. Chem. Eng. Data **33**, 234–237 (1988).
[79]J. G. Baragi, M. I. Aralaguppi, T. M. Aminabhavi, M. Y. Kariduraganavar, and A. S. Kittur, "Density, viscosity, refractive index, and speed of sound for binary mixtures of anisole with 2-chloroethanol, 1,4-dioxane, tetrachloroethylene, tetrachloroethane, DMF, DMSO, and diethyl oxalate at (298.15, 303.15, and 308.15) K," J. Chem. Eng. Data **50**, 910–916 (2005).
[80]T. M. Aminabhavi and K. Banerjee, "Density, viscosity, refractive index, and speed of sound in binary mixtures of 1-chloronaphthalene with benzene, methylbenzene, 1,4-dimethylbenzene, 1,3,5-trimethylbenzene, and methoxybenzene at (298.15, 303.15, and 308.15) K," J. Chem. Eng. Data **44**, 547–552 (1999).
[81]D. R. Lide and H. V. Kehiaian, *CRC Handbook of Thermophysical and Thermochemical Data* (CRC Press, Boca Raton, 2020).
[82]X. Meng, J. Wu, and Z. Liu, "Viscosity and density measurements of diisopropyl ether and dibutyl ether at different temperatures and pressures," J. Chem. Eng. Data **54**, 2353–2358 (2009).
[83]R. C. Reid, "Tables on the thermophysical properties of liquids and gases. 2nd edition, N. B. Vargaftik, Halsted Press, division of John Wiley & Sons, Inc., New York, August, 1975. $49.50, 758 pages," AIChE J. **21**, 1235 (1975).
[84]U. S. P. R. Arachchige, N. Aryal, D. A. Eimer, and M. C. Melaaen, "Viscosities of pure and aqueous solutions of monoethanolamine (MEA), diethanolamine (DEA) and N-methyldiethanolamine (MDEA)," Annu. Trans. Nord. Rheol. Soc. **21**, 299–306 (2013).
[85]C. Yang, H. Lai, Z. Liu, and P. Ma, "Density and viscosity of binary mixtures of diethyl carbonate with alcohols at (293.15 to 363.15) K and predictive results by UNIFAC-VISCO group contribution method," J. Chem. Eng. Data **51**, 1345–1351 (2006).
[86]D. Kodama, M. Kanakubo, M. Kokubo, S. Hashimoto, H. Nanjo, and M. Kato, "Density, viscosity, and solubility of carbon dioxide in glymes," Fluid Phase Equilib. **302**, 103–108 (2011).
[87]P. Zheng, X. Meng, J. Wu, and Z. Liu, "Density and viscosity measurements of dimethoxymethane and 1,2-dimethoxyethane from 243 K to 373 K up to 20 MPa," Int. J. Thermophys. **29**, 1244–1256 (2008).
[88]J. Wu, Z. Liu, S. Bi, and X. Meng, "Viscosity of saturated liquid dimethyl ether from (227 to 343) K," J. Chem. Eng. Data **48**, 426–429 (2003).
[89]L. Sarkar and M. N. Roy, "Density, viscosity, refractive index, and ultrasonic speed of binary mixtures of 1,3-dioxolane with 2-methoxyethanol, 2-ethoxyethanol, 2-butoxyethanol, 2-propylamine, and cyclohexylamine," J. Chem. Eng. Data **54**, 3307–3312 (2009).
[90]B. González, N. Calvar, E. Gómez, and Á. Domínguez, "Density, dynamic viscosity, and derived properties of binary mixtures of methanol or ethanol with water, ethyl acetate, and methyl acetate at T = (293.15, 298.15, and 303.15) K," J. Chem. Thermodyn. **39**, 1578–1588 (2007).
[91]T. Rashid, C. F. Kait, and T. Murugesan, "Effect of alkyl chain length on the thermophysical properties of pyridinium carboxylates," Chin. J. Chem. Eng. **25**, 1266 (2016).
[92]A. G. Ferreira, A. P. Egas, I. M. Fonseca, A. C. Costa, D. C. Abreu, and L. Q. Lobo, "The viscosity of glycerol," J. Chem. Thermodyn. **113**, 162–182 (2017).
[93]H. Freiser and W. L. Glowacki, "Some physical properties of isoquinoline," J. Am. Chem. Soc. **71**, 514–516 (1949).
[94]K. Noda, M. Ohashi, and K. Ishida, "Viscosities and densities at 298.15 K for mixtures of methanol, acetone, and water," J. Chem. Eng. Data **27**, 326–328 (1982).
[95]M. Aralaguppi, C. Jadar, and T. Aminabhavi, "Density, viscosity, refractive index, and speed of sound in binary mixtures of 2-chloroethanol with methyl acetate, ethyl acetate, *n*-propyl acetate, and *n*-butyl acetate," J. Chem. Eng. Data **44**, 441–445 (1999).
[96]N. Chaudhary and A. K. Nain, "Densities, ultrasonic speeds, viscosities, refractive indices, and excess properties of 1-butyl-3-methylimidazolium tetrafluoroborate + *N*-methylacetamide binary mixtures at different temperatures," J. Chem. Eng. Data **65**, 1447–1459 (2020).
[97]K. Narendra, C. Srinivasu, S. Fakruddin, and P. Narayanamurthy, "Excess parameters of binary mixtures of anisaldehyde with o-cresol, m-cresol and p-cresol at T = (303.15, 308.15, 313.15, and 318.15) K," J. Chem. Thermodyn. **43**, 1604–1611 (2011).
[98]R. Rosal, I. Medina, E. Forster, and J. MacInnes, "Viscosities and densities for binary mixtures of cresols," Fluid Phase Equilib. **211**, 143–150 (2003).
[99]M. Yasmin and M. Gupta, "Density, viscosity, velocity and refractive index of binary mixtures of poly(ethylene glycol) 200 with ethanolamine, *m*-cresol and aniline at 298.15 K," J. Solution Chem. **40**, 1458–1472 (2011).
[100]L.-C. Wang, H.-S. Xu, J.-H. Zhao, C.-Y. Song, and F.-A. Wang, "Density and viscosity of (3-picoline + water) binary mixtures from T = (293.15 to 343.15) K," J. Chem. Thermodyn. **37**, 477–483 (2005).
[101]T. M. Aminabhavi, H. T. Phayde, and R. S. Khinnavar, "Densities, refractive indices, speeds of sound and shear viscosities of diethylene glycol dimethyl ether methyl salicylate at temperatures from 298.15 to 318.15 K," Collect. Czech. Chem. Commun. **59**, 1511–1524 (1994).
[102]M. Almasi, "Temperature dependence and chain length effect on density and viscosity of binary mixtures of nitrobenzene and 2-alcohols," J. Mol. Liq. **209**, 346–351 (2015).
[103]A. S. Al-Jimaz, J. A. Al-Kandary, and A.-H. M. Abdul-Latif, "Densities and viscosities for binary mixtures of phenetole with 1-pentanol, 1-hexanol, 1-heptanol, 1-octanol, 1-nonanol, and 1-decanol at different temperatures," Fluid Phase Equilib. **218**, 247–260 (2004).
[104]D. S. Wankhede, M. K. Lande, and B. R. Arbad, "Densities and viscosities of binary mixtures of paraldehyde + propylene carbonate at (288.15, 293.15, 298.15, 303.15, and 308.15) K," J. Chem. Eng. Data **50**, 261–263 (2005).
[105]L. Guinda, J. Santafe, J. Urieta, and C. Gutiérrez Losa, "Viscosity measurements on aniline, p-toludine and p-anisidine + phénol in the temperature range of 303.15–343.15 K," J. Chim. Phys. **83**, 631–636 (1986).

[106]M. Aralaguppi, C. Jadar, and T. Aminabhavi, "Density, viscosity, refractive index, and speed of sound in binary mixtures of acrylonitrile with methanol, ethanol, propan-1-ol, butan-1-ol, pentan-1-ol, hexan-1-ol, heptan-1-ol, and butan-2-ol," J. Chem. Eng. Data **44**, 216–221 (1999).
[107]M. A. Saleh, M. Shamsuddin Ahmed, and S. K. Begum, "Density, viscosity and thermodynamic activation for viscous flow of water+sulfolane," Phys. Chem. Liq. **44**, 153–165 (2006).
[108]C. Yang, P. Ma, and Q. Zhou, "Excess molar volumes and viscosities of binary mixtures of sulfolane with benzene, toluene, ethylbenzene, *p*-xylene, *o*-xylene, and *m*-xylene at 303.15 and 323.15 K and atmospheric pressure," J. Chem. Eng. Data **49**, 881–885 (2004).
[109]P. K. Kipkemboi and A. J. Easteal, "Densities and viscosities of binary aqueous mixtures of nonelectrolytes: *Tert*-butyl alcohol and *tert*-butylamine," Can. J. Chem. **72**, 1937–1945 (1994).
[110]National Center for Biotechnology Information, Pubchem compound summary for cid 6278, 1,1,2,2-tetrachloroethane (accessed 15 October 2024).
[111]T. Savitha Jyostna, B. Satheesh, D. Sreenu, G. Ramesh, G. Sowjanya, and R. Suresh, "Physical-chemical properties of binary liquid mixtures of isoamyl alcohol with chloroethanes at 298–308 K," Russ. J. Phys. Chem. **93**, 278–287 (2019).
[112]V. Antón, H. Artigas, L. Lomba, B. Giner, and C. Lafuente, "Thermophysical properties of the thiophene family," J. Therm. Anal. Calorim. **125**, 509–518 (2016).
[113]S. Kannan and K. Kishore, "Absolute viscosity and density of trisubstituted phosphoric esters," J. Chem. Eng. Data **44**, 649–655 (1999).
[114]D. L. Prak, B. H. Morrow, J. S. Cowart, and J. A. Harrison, "Binary mixtures of aromatic compounds (*n*-propylbenzene, 1,3,5-trimethylbenzene, and 1,2,4-trimethylbenzene) with 2,2,4,6,6-pentamethylheptane: Densities, viscosities, speeds of sound, bulk moduli, surface tensions, and flash points at 0.1 MPa," J. Chem. Eng. Data **65**, 2625–2641 (2020).
[115]E. Carnevale and T. Litovitz, "Pressure dependence of sound propagation in the primary alcohols," J. Acoust. Soc. Am. **27**, 547–550 (1955).
[116]T. Kishimoto and O. Nomoto, "Absorption of ultrasonic waves in organic liquids (II) liquids with negative temperature coefficient of sound absorption (a) glycols, cyclohexanol and cresol," J. Phys. Soc. Jpn. **9**, 1021–1029 (1954).
[117]R. Piccirelli and T. Litovitz, "Ultrasonic shear and compressional relaxation in liquid glycerol," J. Acoust. Soc. Am. **29**, 1009–1020 (1957).
[118]F. H. C. Marriott and J. A. Pope, "Bias in the estimation of autocorrelations," Biometrika **41**, 390–402 (1954).
[119]H. Flyvbjerg and H. G. Petersen, "Error estimates on averages of correlated data," J. Chem. Phys. **91**, 461–466 (1989).
[120]J. Fitzgerald, "Molecular determinants of lipid membrane dynamic properties," Ph.D. thesis, University of Delaware, DE, 2024.
[121]R. Zangi, "Refinement of the OPLSAA force-field for liquid alcohols," ACS Omega **3**, 18089–18099 (2018).
[122]S. Fan, H. Nedev, R. Vijayan, B. I. Iorga, and O. Beckstein, "Precise force-field-based calculations of octanol-water partition coefficients for the SAMPL7 molecules," J. Comput.-Aided Mol. Des. **35**, 853–870 (2021).
[123]C. Vega, J. L. Abascal, M. Conde, and J. Aragones, "What ice can teach us about water interactions: A critical comparison of the performance of different water models," Faraday Discuss. **141**, 251–276 (2009).
[124]S. W. Siu, K. Pluhackova, and R. A. Böckmann, "Optimization of the OPLS-AA force field for long hydrocarbons," J. Chem. Theory Comput. **8**, 1459–1470 (2012).
[125]L. Hall, "The origin of ultrasonic absorption in water," Phys. Rev. **73**, 775–781 (1948).
[126]R. Graves and B. Argrow, "Bulk viscosity: Past to present," in *7th AIAA/ASME Joint Thermophysics and Heat Transfer Conference* (American Institute of Aeronautics and Astronautics, 1998).